الجمهورية الجزائرية الديمقراطية الشعبية

DEMOCRATIC AND POPULAR ALGERIAN REPUBLIC

وزارة التعليم العالي والبحث العلمي

MINISTRY OF HIGHER EDUCATION AND SCIENTIFIC RESEARCH

جامعة الشهيد حمه لخضر الوادي

ECHAHID HAMMA LAKHDAR UNIVERSITY OF EL-OUED

كلية العلوم الطبيعة والحياة

FACULTY OF NATURAL LIFE AND SCIENCES

قسم البيولوجيا الخلوية والجزيئية

Department of Cellular and Molecular Biology

Master 's Thesis

In order to obtain a diploma of an Academic Master In biological sciences

Specialty: Toxicology

Them

Synthesis of Ni(II) and Zn(II) Porphyrin Complexes for Hemoglobin Stabilization and Anti-Hemolytic Activity: In Vitro Studies, ADMET Prediction, Molecular Docking, and Molecular Dynamics An

Presented by:

Mrs. HADJ AMMAR Yousra

Mrs. MENNAI Nihal

Mrs. MESSAI BOUBAKER Soundes

Mrs. RAHAL Amina

Jury Members:

President: Dr. TLILI Mohammed Laid	**El-Oued University**
Examiner: Dr. ALLOUCHE Djenet	**El-Oued University**
Supervisor: Pr. LANEZ Elhafnaoui	**El-Oued University**
Co- Supervisor: Pr. CHAOUA Houssyen	**El-Oued University**

University year: 2024/2025

الاهداء

"من قال أنا لها "نالها

لم تكن الرحلة قصيرة ولا ينبغي لها أن تكون

لم يكن الحلم قريبا ولا الطريق كان محفوفا بالتسهيلات لكنني فعلتها ونلتها

الحمد لله حبا وشكرا وإمتنانا، الذي أنا اليوم أنظر إلى حلم طال انتظاره وقد أصبح واقعا أفتخر به

أهديه إلى من أحمل إسمه وصنعت من ألم غيابه قوة للإستمرار **أبي " خليفة** " الله يرحمك وعوضه أخ والدتي **"الجباري"** أدامه الله تاج فوق رؤوسنا

إلى سندي وقوتي بعد الله، داعمتي الأولى والأبدية **أمي "منصورة"**

أهديك هذا الإنجاز الذي لولا تضحيتكِ لما كان له وجود، ممتنة لأن الله اصطفاك لي من البشر أُما يا خير سند وعوض

وإلى سندي ومسندي وضلعي الثابت الذي لا يميل زوجي **"زواري أحمد رياض"** حفظه الله لي **وإبني الغالي "علي"**

إلى من قال فيهم الله (سنشد عضدك بأخيك)

إلياس الغالي حفظك الله

وإلى من كاتفتني ونحن نشق الطريق إلى من كانت مظلة في أصعب الأوقات صديقتي **"مناعي نهال"**

خريجتكم يسرى.....

الاهداء

الحمد لله الذي بنعمته تتم الصالحات،

الحمد لله الذي بنعمته تتم الصالحات، أهدي تخرجي وثمرة جهدي وذروة سناء دراستي إلى والدي **"مناعي محمد الصغير"**، الذي زين اسمي بأجمل الألقاب، إلى من أحمل اسمه بكل فخر، الذي كان دائمًا ظلًا أستظل به وشرفًا أعتز به.

إن تخرجي اليوم ليس إنجازي وحدي، بل هو ثمرة يدك التي لم تتوقف عن العطاء، وعينك الساهرة، وقلبك الذي لم يعرف إلا الحب.

أهدي تخرجي إلى والدتي الراحلة **"ذهب مرزاقة"** (رحمها الله)، ثمرة جهودي، والفرح الذي طالما انتظرته، إلى أمي التي كان حلمها أن تراني أتخرج قبل أن ترحل عن هذه الدنيا. لكنها تبقى حيةً في قلبي، ولا تزال دعواتها ترافقني في كل خطوة، وهذا الإنجاز... لكِ أولًا وأبدًا.

إلى دعمي الدائم، وسندي الذي لا يهتز - إخوتي:

"ياسين" "صلاح الدين" "عز الدين" "عمار"

و إلى أخواتي، نبض روحي وأجمل عطايا حياتي،

إلى من كانت قلوبهم موطنًا للحنان، وأياديهم عونًا في كل طريق،

أهديكم ثمرة تعبي، فبكم كان للحلم معنى وللرحلة طعم أجمل،

أحبكم بلا حدود، ودعائي أن تبقوا نور أيامي إلى : **"مروى" "إسراء" "جوري"**

إلى صديقتي الأبدية، التي شاركتني سنوات الدراسة، والتي ولدتها لي الحياة : **"حاج عمار يسرى "**

أتقدم بجزيل الشكر لأستاذي فاضل الدكتور **(العانز الحفناوي)**

على دعمه القيم، وتوجيهه، وجهوده أثناء إعداد مذكرة التخرج. لقد كان دعمك أثر كبير ، وأتقدم لك بأصدق مشاعر التقدير وأطيب التمنيات بمزيد من النجاح المستمر

"الخريجة نهال "

الاهداء

إلى والديّ العزيزين

أتقدم بجزيل الشكر والامتنان والحب والتقدير لوالديّ، شعاع الشمس الذي أتشبث به كل يوم. أشكركما على كل الدعم والتشجيع الذي قدمتماه لي طوال مسيرتي الدراسية. حفظكما الله وأدام عليكما الصحة والعافية.

إلى أستاذي الفاضل **"العانز الحفناوي""**

الذي كان الشرف الكبير بأن يتولى الإشراف على هذه الدراسة، والذي منحني ثقته ولم يبخل علي بنصائحه القيمة.

إلى جدتي

حفظك الله ورزقك عمرًا مديدًا مليئًا بالسعادة والصحة.

إلى إخوتي وأخواتي

لطالما ساعدتموني ودعمتموني. هذه السطور القليلة لا تكفي للتعبير عن امتناني لكل ما قدمتموه. بارك الله فيكم وحفظكم.

إلى أعمامي وخالاتي الأعزاء

الذين وقفوا بجانبي دائمًا في السراء والضراء.

إلى عائلتي الكبيرة رب

تعبيرًا عن احترامي ومحبتي.

إلى زملائي طلاب دفعة 2025 في علم السموم الأساسي - تخليدًا لذكرى اللحظات الرائعة التي جمعتنا

الخريجة سندس.....

الاهداء

الحمد لله الذي بنعمته تتم الصالحات، الحمد لله عدد ما كان و عدد ما يكون، الحمد لله الذي وفقني وأعانني على إتمام هذا العمل رغم التحديات.

واحمدك يارب على كل لحظة تعب أثمرت، وعلى كل طريق سلكته وكنت فيه معي

و أصلي وأسلم على سيدنا محمد خير من علم وأرشد وعلى اله وصحبه أجمعين.

الى من كانوا أمان القلب ، وسند الروح وترياق كل تعب :

الى أمي التي كانت دعاؤها ملاذي في كل ليل,

الى أبي الذي أحمل اسمه بكل فخر والذي علمني أن الطريق يبدأ بالايمان وينتهي بالنجاح .

الى اشقاء الروح جسر المحبة والوفاء اخوتي واخواتي كل واحد باسمه

أتقدم بجزيل الشكر والامتنان الى أستاذي المشرف **"العانز الحفناوي"** ،على ما بذله من جهد، وتوجيه ،ونصح طيلة فترة انجاز هذه المذكرة، فلولا دعمه العلمي والمعنوي لما تمكنا من الوصول الى هذه النتيجة .

الى زملاء الرحلة، من خضنا معا تجارب المختبر، وتقارير السموم، وضغط الامتحانات ، من علموني ان المعرفة تشارك ، وان العلم رحلة جماعية...

في علم السموم تعلمت أن لكل سم دواء، وكذلك في الحياة، لكل ألم شفاء...

الى من كانوا ترياقي في أوقات ضعفي، وعزائي في لحظات تعبي

أهدي هذا العمل المتواضع، راجية من الله ان يكون هذا العمل إضافة تخدم تقدم البحث العلمي، وأن يجعل هذا الجهد أول خطوة في مسيرة علمية وعملية مباركة، مليئة بالعطاء والنجاح ... بكل فخر وامتنان،

الخريجة امينة.....

شكر وتقدير

بسم الله الرحمن الرحيم

الحمد لله الذي بنعمته تتم الصالحات، وبفضله أنجزنا هذا العمل المتواضع.

نتقدم نحن، بخالص عبارات الشكر والتقدير لكل من كان له دور في دعمنا ومساندتنا خلال سنوات الدراسة وحتى إنجاز هذه المذكرة.

شكرًا لأساتذتنا الأفاضل على كل ما قدموه لنا من علم ومعرفة، وعلى توجيهاتهم السديدة وملاحظاتهم القيمة.

شكر خاص نقدمه إلى عائلاتنا الكريمة، التي كانت السند الحقيقي والداعم الأول لنا، وإلى كل من مدّ لنا يد العون بكلمة مشجعة أو دعوة صادقة.

كما لا ننسى أن نشكر أنفسنا وصديقاتنا العزيزات على روح التعاون، والمثابرة، والدعم المتبادل الذي كان نورًا يضيء طريقنا طوال هذه الرحلة.

لكم جميعًا أصدق مشاعر الشكر والعرفان، سائلين الله دوام النجاح والتوفيق في حياتنا وحياة من أحببناهم

.....

Abstract

This study aims to investigate the effect of four porphyrin derivatives on hemoglobin, given the importance of their ability to bind to heme-containing proteins and influence their functions. The research focused on evaluating the potential of these four porphyrin derivatives as therapeutic agents by assessing their ability to modulate oxidative stress and hemolysis. In vitro experiments were conducted, and the chemical structures of the compounds were confirmed using various analytical techniques, including cyclic voltammetry, UV-Vis spectroscopy, and nuclear magnetic resonance (NMR).

The results showed that all four derivatives bind to hemoglobin with varying degrees of effectiveness. The compound $TbiPPH_2$ exhibited the strongest binding, with an IC_{50} value of 28.57 µg/mL, while $ZnTPPH_2$ showed the weakest (IC_{50} = 45.95 µg/mL). In terms of binding constants and free energy, $NiTPPH_2$ demonstrated the highest binding constant and the most favorable ΔG value (-23.48 kJ/mol), indicating a strong and spontaneous interaction. Regarding anti-hemolytic activity, $NiTPPH_2$ also showed the lowest half-maximal inhibitory concentration (IC_{50}), followed by $TPPH_2$.

Molecular docking simulations supported these findings, revealing stable interactions with hemoglobin, with $NiTPPH_2$ being the most stable, showing a ΔG value of -31.12 kJ/mol, in agreement with the experimental data. Porphyrin derivatives, particularly $NiTPPH_2$, exhibit strong binding to hemoglobin and offer effective protection against hemolysis, making them promising candidates for therapeutic applications targeting oxidative stress and the preservation of red blood cells.

Keywords: TbiPPH2, ZnTPPH2, NiTPPH2, $TPPH_2$, hemolysis, hemoglobin, IC_{50}, porphyrin derivatives

RÉSUMÉ

Cette étude vise à étudier l'effet de quatre dérivés de la perforine sur l'hémoglobine, étant donné l'importance de sa capacité à se lier aux protéines contenant le groupe hème et à affecter leurs fonctions. Ce problème tournait autour de la connaissance du potentiel des quatre dérivés de la perforine en tant qu'agents thérapeutiques en évaluant leur capacité à modifier le stress oxydatif et l'hémolyse. Des expériences en laboratoire ont été menées (in vitro) et les structures chimiques de ces composés ont été confirmées à l'aide de plusieurs techniques analytiques, notamment : la voltamétrie cyclique, la spectroscopie UV-Vis et la résonance magnétique nucléaire. Les résultats ont montré que les quatre dérivés se lient à l'hémoglobine avec des degrés d'efficacité variables. TbiPPH2 a enregistré la liaison la plus forte avec une valeur IC50 de (28,57 µg/ml), tandis que ZnTPPH2 était la plus faible (45,95 µg/ml). En termes de constantes de liaison et d'énergie libre, NiTPPH2 a montré la valeur de constante de liaison la plus élevée et la meilleure valeur ΔG de (-23,48 kJ/mol), indiquant une interaction forte et spontanée. En ce qui concerne l'activité antihémolytique, NiTPPH2 avait également la CI50 la plus faible, suivie de TPPH2. Les simulations d'amarrage moléculaire ont soutenu ces résultats, montrant des interactions stables avec l'hémoglobine, NiTPPH2 étant le plus stable avec une valeur de ΔG = 31,12 kJ/mol, ce qui est en accord avec les données expérimentales. Les dérivés de la perforine, en particulier Nitpph2, forment une forte affinité de liaison à l'hémoglobine et ces composés présentent une protection efficace contre l'hémolyse. Ces résultats en font des candidats prometteurs pour des applications thérapeutiques ciblant le stress oxydatif et la préservation des globules rouges.

Mots clés : le stress oxydatif, l'hémolyse, l'hémoglobine, l'IC_{50} et les dérivés de porphyrine

الملخص

تهدف هذه الدراسة إلى دراسة تأثير أربعة مشتقات من البرفورين على الهيموغلوبين نظرا لأهمية قدرته على الارتباط بالبروتينات المحتوية على مجموعة الهيم و التأثير على وظائفها، إذ تمحورت هذه الإشكالية حول معرفة إمكانيات مشتقات البرفورين الأربعة كعوامل علاجية من خلال تقييم قدرتها على تعديل الإجهاد التأكسدي والانحلال الدموي، حيث اجريت تجارب مخبرية(In Vitro) و تم تأكيد البنية الكيميائية لهذه المركبات باستخدام تقنيات تحليلية متعددة منها: الفولتميتر الدوري - التحليل الطيفي للاشعة فوق البنفسجية و المرئية - الرنين المغناطيسي النووي.أظهرت النتائج أن جميع المشتقات الأربعة ترتبط بالهيموغلوبين بدرجات متفاوتة من الفعالية، حيث سجل مركب TbiPPH2 أقوى ارتباط بقيمة IC50 بلغت (28.57 ميكروغرام / مل)، في حين كان ZnTPPH2 الأضعف (45.95 ميكروغرام / مل). من حيث ثوابت الارتباط والطاقة الحرة، فأظهر NiTPPH2 أعلى قيمة ثابت ارتباط وأفضل قيمة Δ G بلغت (23.48- كيلوجول/مول)، مما يشير إلى تفاعل قوي وتلقائي. وفيما يخص النشاط المضاد للانحلال الدموي، تميز NiTPPH2 أيضًا بأقل تركيز مثبط نصف أعظمي (IC_{50}) يليه مركب TPPH2، دعمت عمليات محاكاة الالتحام الجزيئي هذه النتائج، حيث أظهرت تفاعلات مستقرة مع الهيموغلوبين ، وكان NiTPPH2 الأكثر استقرارًا بقيمة بلغت (31.12-= ΔGكيلوجول /مول)، مما يوافق البيانات التجريبية. تشكل مشتقات البرفورين وخاصة Nitpph2 ارتباطا قويا بالهيموغلوبين وتظهر هذه المركبات حماية فعالة ضد الانحلال الدموي، هذه النتائج تجعلها مرتبطة واعدة للتطبيقات العلاجية التي تستهدف الإجهاد التأكسدي والحفاظ على الخلايا الدم الحمراء.

الكلمات المفتاحية: الاجهاد التأكسدي، الانحلال الدموي، الهيموغلوبين، IC_{50}، مشتقات البرفورين

ABBREVIATIONS LIST

13C NMR; Carbon-13 Nuclear Magnetic Resonance

1H NMR; Proton Nuclear Magnetic Resonance

BpG; 2,3-Bisphosphoglycerate

COHb; Carboxyhemoglobin

DDQ; 2,3-Dichloro-5,6-dicyano-1,4-benzoquinone

DFT; Density Functional Theory

DMF;Dimethylformamide

Dpph; 2,2-Diphenyl-1-picrylhydrazyl

FHb; Free Hemoglobin

Hb ;Hemoglobin

HbO2; Oxyhemoglobin

HHb; Human Deoxyhemoglobin

IC50; Inhibitory Concentration 50%

LDH ;Lactate Dehydrogenase

MD; Molecular Dynamics

MetHb; Methemoglobin

MM ; Molecular Mec

NIRS; Near-Infrared

NMR ;Nuclear Magnetic Resonance

NO; Nitric Oxide

R; Relaxed state

RBCs; Red Blood Cells

ROs; Reactive Oxygen Species

Spectroscopy

T; Tense state

TFA;Trifluoroacetic Acid

TLRs; Toll-Like Receptors

TPP; Tetrapheny|porphyrin

UV-Vis ; Ultraviolet-Visible Spectroscopy

VTRs; Vascular Tone Regulato

FIGURES LIST

TABLES LIST

Summary

Introduction

Introduction

In recent years, the development of novel compounds with antioxidant and anti-hemolytic properties has garnered significant attention due to the increasing recognition of oxidative stress and hemolysis as underlying factors in a variety of diseases. Porphyrins, a class of compounds characterized by their distinct macrocyclic structure comprising four pyrrole rings linked by methine bridges, have emerged as promising candidates in this domain due to their versatile chemical properties. These compounds exhibit intrinsic antioxidant activity, which is attributed to their ability to scavenge reactive oxygen species (ROS) and neutralize oxidative stress. Additionally, emerging studies suggest that certain porphyrins demonstrate anti-hemolytic effects, highlighting their potential therapeutic applications in protecting red blood cells from damage. [95]

Porphyrins have long been studied for their interactions with biological macromolecules, particularly proteins such as hemoglobin (HHb), due to their ability to bind to heme-containing proteins and affect their functionality. Understanding these interactions is crucial for designing molecules that can modulate hemoglobin behavior, which is relevant in conditions such as anemia and other hemolytic disorders. Moreover, the molecular docking of porphyrins with hemoglobin has provided valuable insights into the ligand-receptor binding modes, which may aid in optimizing the efficacy of porphyrin-based therapeutic agents.

In this study, we focus on the synthesis, characterization, and evaluation of four porphyrin derivatives: Nickel tetraphenyl-porphyrin ($NiTPPH_2$), meso-tetraphenyl-porphyrin ($TbiPPH_2$), meso-tetramethophenyl-porphyrin ($TPPH_2$ (o-methyl)), and Zinc-tetra4-methophenyl-porphyrin ($ZnTPPH_2$ (p-methyl)). These derivatives were investigated for their antioxidant and anti-hemolytic properties through both in vitro and in silico methods. The antioxidant capacity of these compounds was assessed using electrochemical and spectroscopic techniques, including cyclic voltammetry and UV-Vis spectroscopy. Furthermore, molecular docking studies were conducted to predict the binding affinities of these porphyrins with hemoglobin, and to understand the interaction dynamics at the molecular level.

The objective of this thesis is to explore the potential of these four porphyrin derivatives as therapeutic agents by assessing their ability to modulate oxidative stress and hemolysis. This will be achieved through a combination of experimental and computational approaches, including electrochemical assays, spectroscopic analysis, and molecular docking simulations. The results obtained from these methods will provide valuable insights into the interactions

between porphyrins and hemoglobin, contributing to the development of new strategies for managing oxidative stress-related disorders.

This research was conducted at the VTRS laboratory of El Oued University, and it aims to contribute significantly to the understanding of porphyrin-based molecules as potential therapeutic agents. The structure of the thesis is organized as follows:

- Provides an introduction to porphyrins, antioxidants, anti-hemolytic mechanisms, and their relevance to hemoglobin interactions.
- Outlines the analytical methods used to assess the HHb and anti-hemolytic properties of the porphyrins, including electrochemical and spectroscopic techniques.
- Focuses on the experimental evaluation of the HHb capacity of the porphyrins.
- Discusses the anti-hemolytic efficacy of the porphyrins, with a focus on the results from electrochemical, spectroscopic, and molecular docking studies.
- Provides an overview of the experimental techniques employed throughout the study.
- Finally, the conclusions will summarize the key findings of the research and suggest potential future directions for this work.

.

First part

BIBLIOGRAPHY

Chapter I

Porphyrins

I.1. General Information on porphyrins:

I.1.1. Definition, properties and applications of porphyrins:

Porphyrin is a macrocycle composed of four pyrrolic units linked together by methene bridges. These bridges form the four meso positions of the porphyrin, while the carbon atoms carried by the four pyrroles constitute the α and β positions (Figure I.1). This molecule possesses 22 π electrons, 18 of which participate in its aromaticity, as dictated by Hückel's rule of 4n + 2 delocalized electrons, where in this case, n equals 4. The completely unsubstituted form of porphyrin is referred to as porphine.[1]

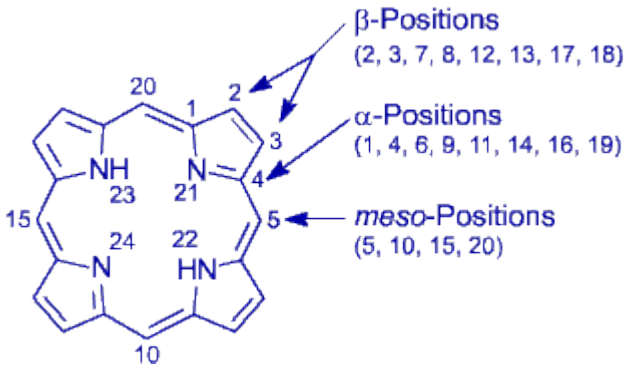

Figure I.1. Structure of porphine [2]

Porphyrin can be found in the so-called 'freebase' form (Figure I.1) or in a metal-complexed form, wherein a metal cation, typically with an oxidation state of (+II) or (+III), is coordinated (Figure I.2)

Figure I.2. Metalized porphine (M = metal) [3]

Porphyrins cover a wide field of applications. Heme, a naturally occurring iron porphyrin found in hemoglobin, plays a crucial role in oxygen transportation within the body. Chlorophyll, another naturally existing porphyrin, is integral to the mechanisms of photosynthesis. Porphyrins find utility in various fields, including photodynamic therapy, biosensors, redox

catalysis, artificial photosynthesis, the design of photovoltaic cells, nonlinear optics, and molecular recognition.

I.1.2. Spectroscopic and electrochemical characterizations of porphyrins:

1.1.2.1. NMR nuclear magnetic resonance:

1.1.2.1.1. Proton NMR spectroscopy (1H NMR):

Proton nuclear magnetic resonance applied to porphyrin macrocycles has two characteristic signals. The meso positions and the α and β positions appear.

Pyrrolic β protons around 8-9 ppm. The multiplicity of these protons depends on the symmetry of the porphyrin and the nature of the substituents in the meso position.

The protons of the pyrrolic nitrogens are around -2ppm. These protons are exchangeable and form a broad signal .

Due to the aromatic structure of the porphyrin nucleus, the core protons are inducted into a very strong shielding cone. The cycle current generated by the magnetic field induces a large cone of magnetic anisotropy whose axis is perpendicular to the plane of the macrocycle. Thus the protons inside this cone (H of pyrrolic nitrogens) are shielded around 3ppm while the portons located outside (H. β .pyrrolic) are strongly deshielded [4].

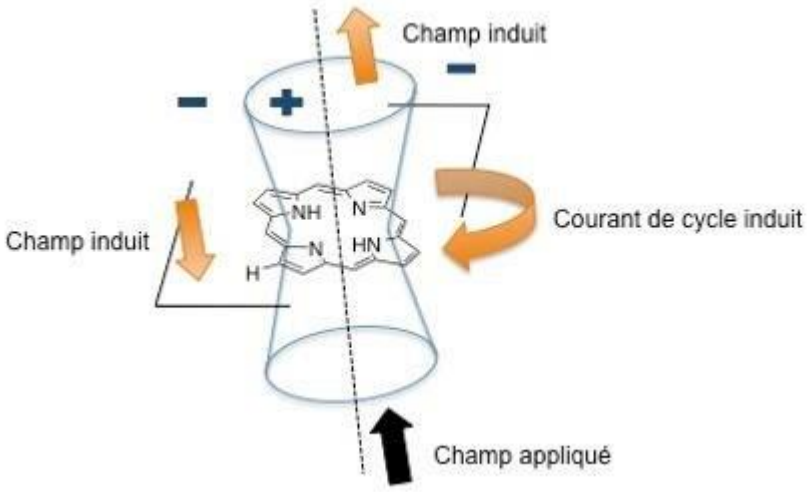

Figure I.3. Anisotropy magnetic cone of a porphyrin [5]

The 1H NMR spectrum of porphine (porphyrin without any substituent) consists of three singlets at -3.76, 9.74, and 10.50 ppm [3]. These signals are attributed respectively to the protons bound to nitrogen atoms, the protons in the β-pyrrolic positions, and the methine protons (meso position). Since the latter are attached to carbons that are essentially electron-deficient, they are more deshielded than the β-pyrrolic protons. Moreover, the uniqueness of the β-pyrrolic proton signals is explained by the tautomerism of the internal NH protons. [6] , Figure 1.4.

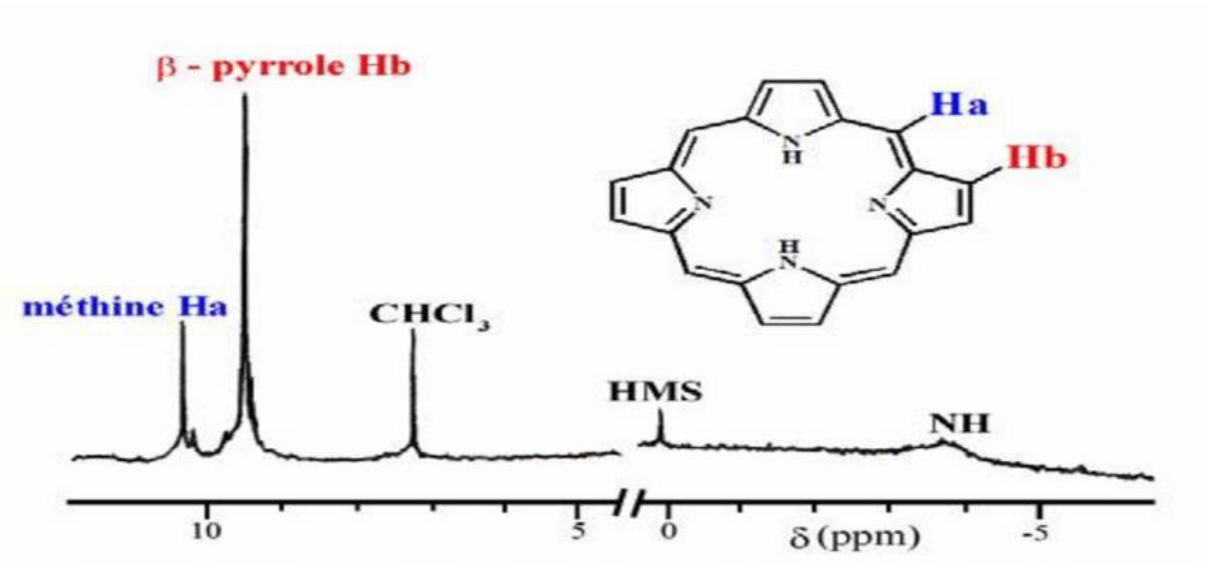

Figure.I.4. [1]H NMR spectrum of porphyrin in CHCl3 [7]

I.1.2.1.2. Carbon-13 NMR Spectroscopy ([13]C NMR) :

The [13] C NMR of the porphyrin could be split into three different areas: alpha pyrrolic, betapyrrolic, and meso carbons. Regarding the first two types, alpha, and beta, there's a problem in discovering obviously their related peaks credited to NH tautomerism. These indicators are clearer at low temperatures since NH tautomerism is sluggish as temperature lowers.

Normally, alpha carbons are found at around 145 ppm. Furthermore, there's a fairly continuous chemical substance change (about 17 ppm) difference between your alpha carbon indicators. Regarding beta carbons, they have emerged at around 130 ppm. The chemical substance shift difference between your beta carbons is smaller than that in case there is alpha. It differs between 5.3 and 6.9 ppm. For meso carbons, they are usually between 95 and 120 ppm.If porphyrin primary is metallated, the indicators of alpha and beta carbons will be upshifted. On the other hand, meso carbons show downfield shifts . [8]

I.1.2.2. UV-Visible Spectroscopy :

In the UV-visible spectrum of porphyrins, two distinct absorption bands are discernible, originating from distinct electronic transitions. Porphyrins possess a highly conjugated p-electron system [9], leading to their absorption within the visible spectrum and the manifestation of a characteristic absorption pattern. This pattern arises from transitions: p → p*, characterized by a prominent band (with an extinction coefficient exceeding 100000 L.mol-1.cm-1) positioned between 390 and 430 nm (near UV), known as the Soret band or B band [10], accompanied by four additional bands spanning from 480 to 700 nm (Visible). Each of these bands exhibits intensities approximately ten to twenty times lower and is designated as a Q band.

The spectral range within the visible spectrum, typically responsive to structural changes, offers insights into macrocycle substitutions. Specifically, the four Q bands, designated from I to IV based on their ascending energy levels, exhibit significant variations in relative intensities contingent upon the identity and placement of the substituent [11].

There are essentially four types, called etio, rhodo, oxorhodo, and phyllo [12].

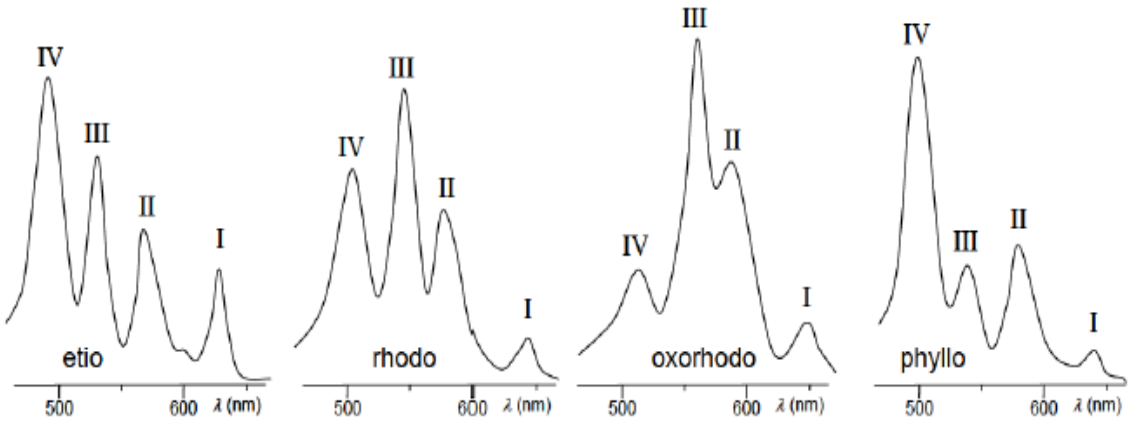

Figure I.5. Different Q bands of free base porphyrins [13]

1.1.2.3. Cyclic Voltammetry:

The electrochemical behavior of porphyrin depends on its free base or metal form, the substitution of the macrocycle, and the solvent used for the study. The most porphyrinstudied is tetraphenyl porphyrin (TPP).

The electrochemical examination of free-base porphyrins typically reveals two stages of single-electron oxidation and two to four stages of single-electron reduction [14-17]. Initially, the porphyrin's first oxidation leads to the forming of a radical cation [18], which subsequently transforms into a dication during the second oxidation stage of the macrocycle. In the reduction process, an anion radical is generated initially, followed by the formation of a di-anion after the first two reduction stages. Notably, the electrochemical reduction of TPP demonstrates that the third and fourth stages of porphyrin reduction are characterized by increased complexity [19,20].

The cation radicals obtained after the first-stage oxidation of free base porphyrins are known to be highly reactive, leading to the protonation of the porphyrin[21].

In 1998, Yves Le Mest and his collaborators published a proposed mechanism for the protonation of TPP through oxidation (Scheme.I.1). In the case of TPP, the monoprotonated form is found to be unstable. Consequently, the deprotonation product is achieved after the

abstraction of two-electron equivalents. The hydrogen radicals likely originate from the solvent used.

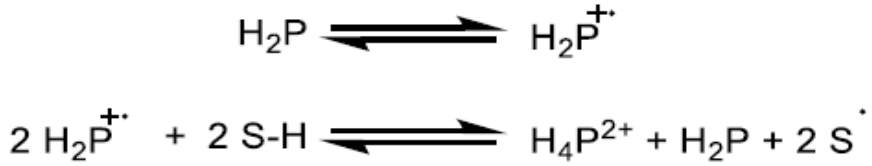

Schema I.1. Proposed mechanisms for the protonation of TPP during their first-stage oxidation [22]

For metalloporphyrins containing a non-electroactive metal cation, such as those metallated with Zn(II) or Mg(II), the redox behavior observed through cyclic voltammetry is similar to that of free base porphyrins. The presence of the metal primarily influences the oxidation and reduction potentials of the macrocycles. These potential values are directly correlated with the electronegativity of the metal incorporated into the metalloporphyrin.[23]The higher the electronegativity of the metal within the metalloporphyrin, the easier the oxidation, and the more challenging the reduction process.[24]

In the 1970s, Fuhrhop and his collaborators asserted that the potential difference between the first oxidation and first reduction of a porphyrin (Δ|Red1-Ox1|) is 2.25 ± 0.15 V. Additionally, they demonstrated that the first and second oxidations of porphyrin are consistently separated by a potential difference of approximately 0.3 ± 0.1 V (Δ|Ox2-Ox1|), and that the first and second reductions of the macrocycle are separated by approximately 0.4 ± 0.1 V (Δ|Red2-Red1|) [25] (Figure.I.6). It's important to note that these findings hold only for porphyrins with a non-electroactive metal cation at the center.

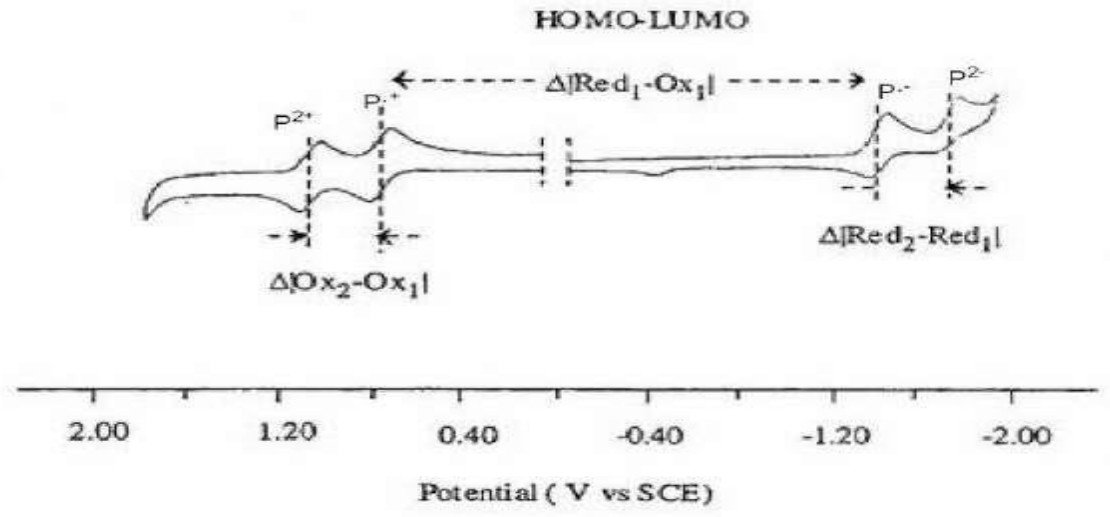

Figure I.6. Cyclic voltammetry of TPP in CH2Cl2.[26]

I.1.3. Description of porphyrin synthesis pathways :

Porphyrins can be synthesized by the condensation of pyrrole with an aldehyde in the presence of an acid and an oxidant (method of Rothemund). The preparation of porphyrins substituted in the meso position and/or the β position of porphine, and more particularly the mechanism of porphyrin formation, have been the subject of a large number of studies.

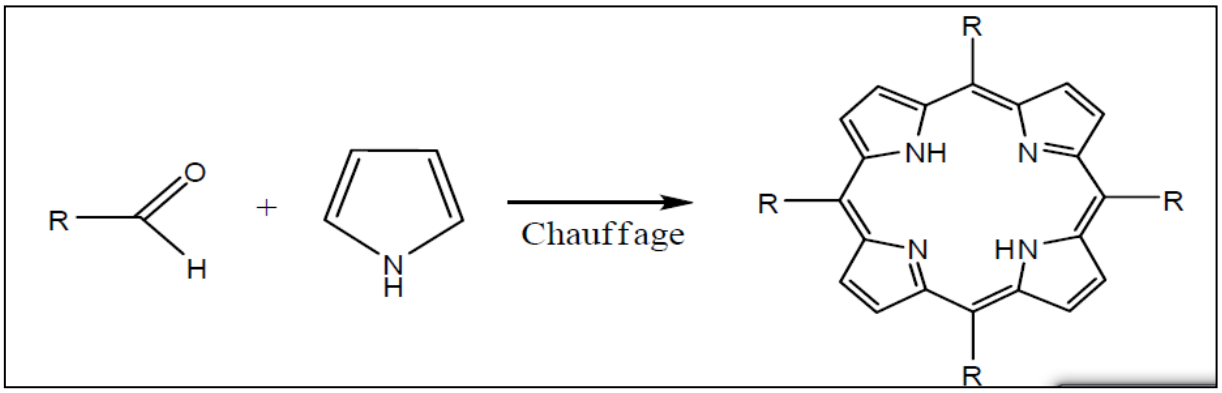

Figure I.7. Method of Rothemund[27]

The most extensively studied porphyrin is TPP. Its synthesis, as demonstrated by Adler and Longo in 1967, is influenced by several factors including medium acidity, solvent choice, reaction temperature, oxygen availability, and initial reagent concentration. Through various investigations, the most effective synthesis method was determined: condensing four equivalents of pyrroles with benzaldehyde at reflux in propionic acid (141°C), resulting in TPP with yields around 20% in crystalline form and reproducibly. [28–31]

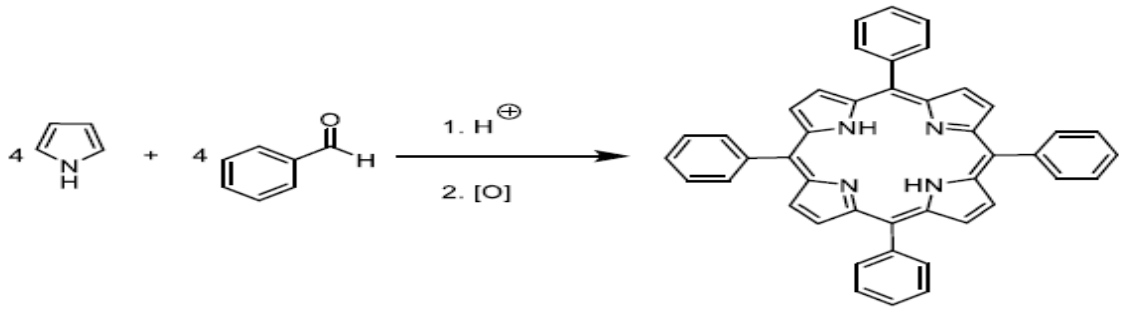

Figure I.8. Method of Adler and Longo [32]

Lindsey and his collaborators also contributed to refining the method proposed by Adler and Longo. [33–36] Pyrrole is condensed with the aldehyde in a chlorinated solvent (dichloromethane or chloroform) in the presence of a catalytic amount of trifluoroacetic acid (TFA) or $BF_3 \cdot (Et)_2O$ at room temperature. The resulting porphyrinogen is then oxidized with an oxidant such as 2,3-dichloro-5,6-dicyano-1,4-benzoquinone (DDQ) to yield meso-tetrasubstituted porphyrins, with a yield ranging between 30% and 40%.

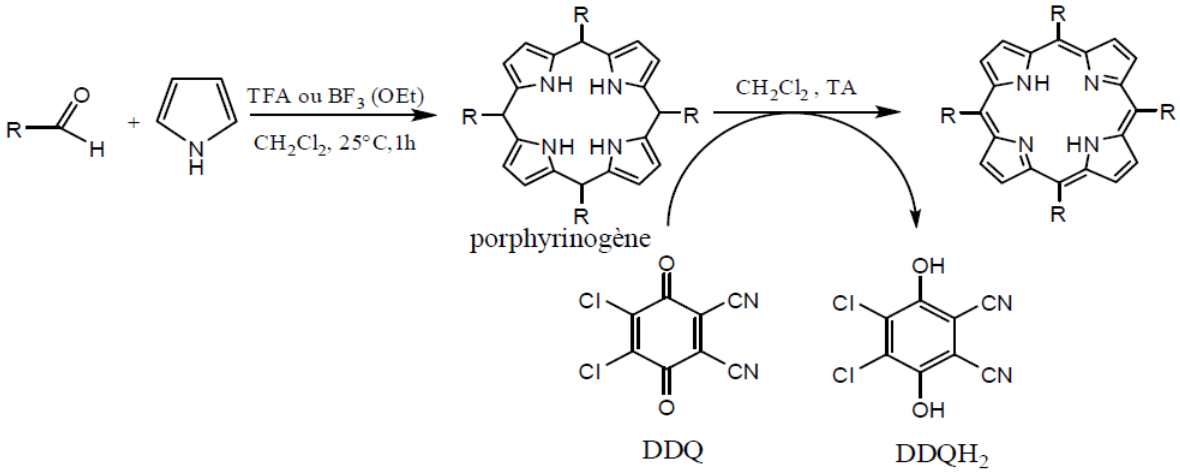

Figure.I.9. Method of Lindsey[37]

MacDonald describes a more targeted synthesis route in three stages, [38] as illustrated in Figure 1.10. The first step of the synthesis involves dipyrromethane, which is produced from the reaction of an aldehyde with an excess of pyrrole. Alternatively, it is possible to use multiple aldehydes and dipyrromethanes in the same so-called [2+2] condensation reaction by MacDonald. [39]

The main drawback of this type of condensation is the formation of statistical mixtures of isomers, which can prove challenging to separate and inevitably reduce yields if only one of the isomers is desired. [40]

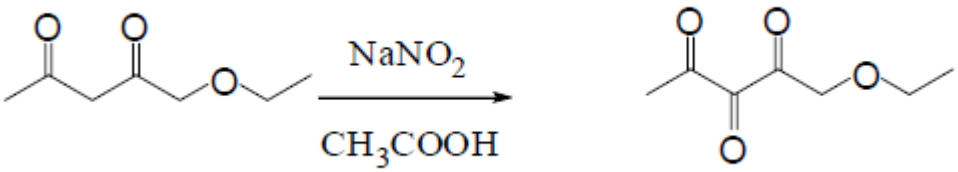

Figure.I.10. Method Mac Donald [41]

The introduction of functional groups at the β-pyrrolic positions is commonly achieved through the preparation of pre-functionalized pyrrolic intermediates. These intermediates encompass both basic pyrroles, referred to as dipyrromethanes, and more complex structures like a,c-diladienes, which represent oligomeric forms of four pyrroles. By systematically incorporating diverse functional moieties under controlled conditions, modified porphyrin derivatives can be synthesized.

One of the notable synthesis methods is the Knorr method, which produces highly functionalized pyrroles from basic substrates [42]. Knorr's method, dating back to 1884,

involves the stoichiometric combination of ethyl acetoacetate with an oxime, prepared through treatment with sodium nitrite, and subsequently reduced by zinc in acetic acid.(Figure.I.11)

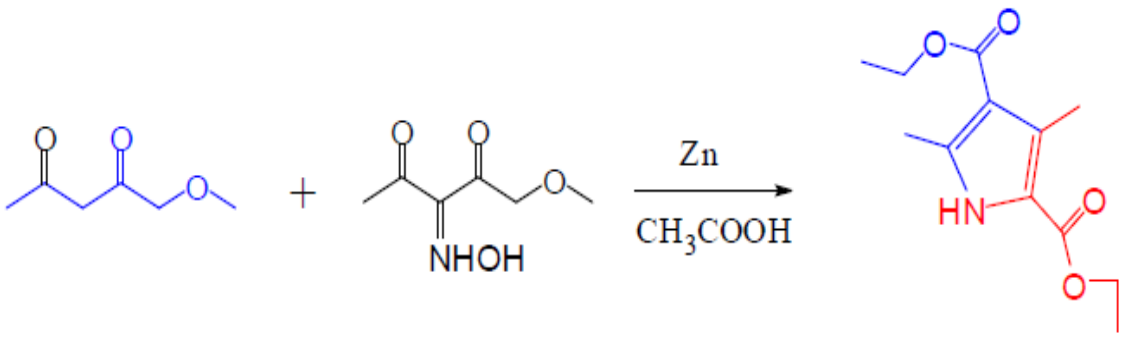

Figure.I.11. Method of Knorr [43]

Another significant method for pyrrole synthesis is the Barton-Zard method. This method entails the use of a nitroacetate, which, upon deprotection of the acetate group in the presence of a base, generates a nitroalkane. Subsequent reaction with a derivative of isocyanoacetate leads to cyclization, resulting in the desired pyrrole after elimination of the nitro NO_2 group. [44]

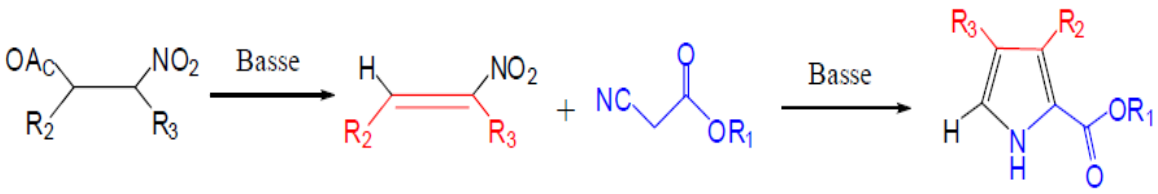

Figure I.12. Method of Barton-Zard [45]

Chapter II Hemoglobin and Hemolysis

1.1 Introduction

Red blood cells (RBCs), or erythrocytes, are highly specialized cells responsible for the transport of respiratory gases throughout the body. Their primary functional component, hemoglobin (Hb), is a tetrameric protein composed of heme prosthetic groups embedded within globin chains, enabling efficient oxygen binding and delivery to tissues. The structural integrity and physiological function of hemoglobin are essential for maintaining cellular respiration and overall metabolic homeostasis.

Among the various physiological and pathological alterations that affect red blood cells, hemolysis represents a critical process characterized by the premature rupture of erythrocytes and the subsequent release of hemoglobin into the plasma. This phenomenon can occur under a wide range of conditions, including mechanical stress, oxidative damage, infections, genetic disorders, or exposure to exogenous agents such as drugs and chemical compounds.

Hemolysis, particularly when uncontrolled or extensive, is associated with significant clinical consequences, including anemia, inflammation, and organ dysfunction. Furthermore, the release of hemoglobin and heme into the extracellular environment contributes to oxidative stress and inflammatory cascades, exacerbating cellular damage.

Understanding the biochemical and structural dynamics of hemoglobin, especially its deoxygenated form (HHb), and the molecular mechanisms underlying hemolysis is crucial for evaluating the potential impact of exogenous compounds, such as porphyrin derivatives, on erythrocyte stability and viability. This chapter provides a detailed overview of hemoglobin structure and function, the nature and consequences of hemolysis, and the analytical approaches employed to study these processes in biomedical research.

1.2 Structure and Function of Hemoglobin

Hemoglobin (Hb) is the principal oxygen-carrying metalloprotein found in red blood cells, accounting for nearly one-third of the cell’s volume. It plays a fundamental role in the transport of oxygen from the lungs to peripheral tissues and the return of carbon dioxide for exhalation. Hemoglobin’s function is tightly linked to its complex quaternary structure, which allows cooperative binding and release of oxygen molecules in response to physiological needs.[46]

1.2.1 Molecular Structure of Hemoglobin

The hemoglobin molecule is a heterotetrametric composed of two α (alpha) and two β (beta) globin chains, each associated with a prosthetic heme group. Each globin chain consists of approximately 141–146 amino acids folded into a globular configuration that stabilizes the

heme pocket. The heme group itself is a protoporphyrin IX ring coordinated to a central iron (Fe^{2+}) atom, which serves as the active site for reversible oxygen binding.

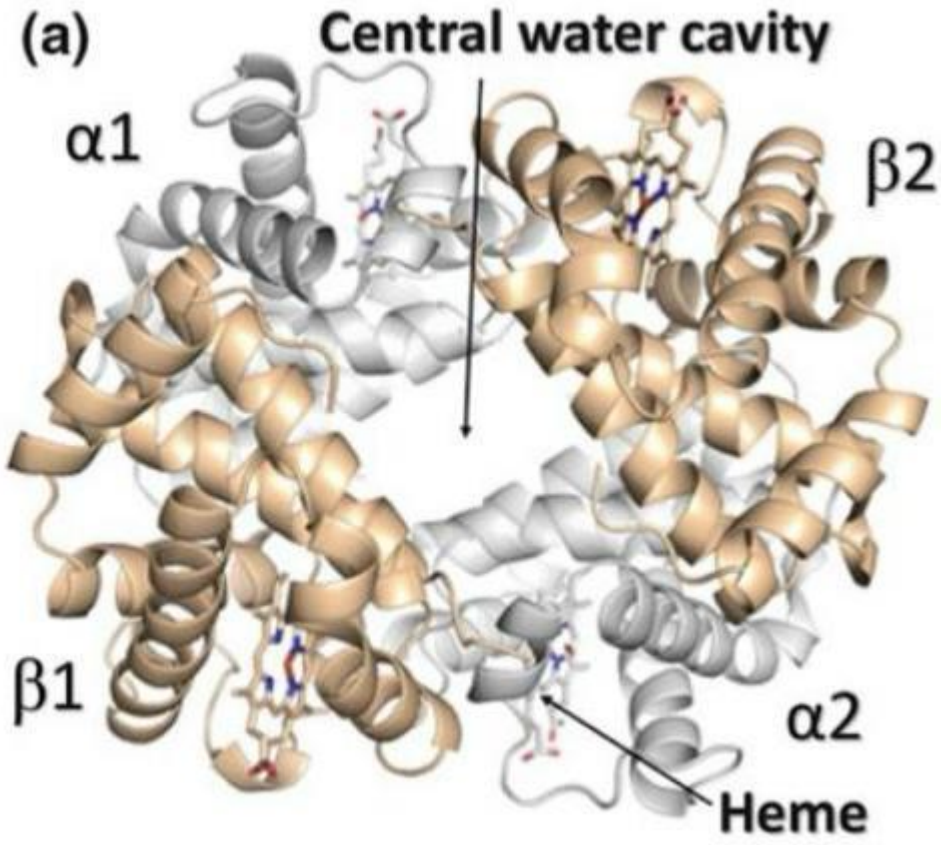

Figure II.1. Schematic representation of human hemoglobin tetramer, composed of two α-globin and two β-globin chains. Each subunit contains one heme prosthetic group. [47]

The iron atom in the heme group coordinates with four nitrogen atoms of the porphyrin ring in the plane, one proximal histidine residue from the globin protein, and a sixth coordination site available for binding oxygen. This geometry is crucial for hemoglobin's ability to bind and release oxygen without undergoing irreversible oxidation.[48]

1.2.2 Oxygen Binding and Allosteric Regulation

Hemoglobin exhibits cooperative binding behavior, a property known as allosterism. When one oxygen molecule binds to a heme group, the entire hemoglobin tetramer undergoes a conformational shift from the tense (T) state to the relaxed (R) state, which increases the affinity of the remaining subunits for oxygen. This sigmoidal binding curve enables hemoglobin to efficiently pick up oxygen in the lungs and release it in tissues where the partial pressure of oxygen is lower.[49]

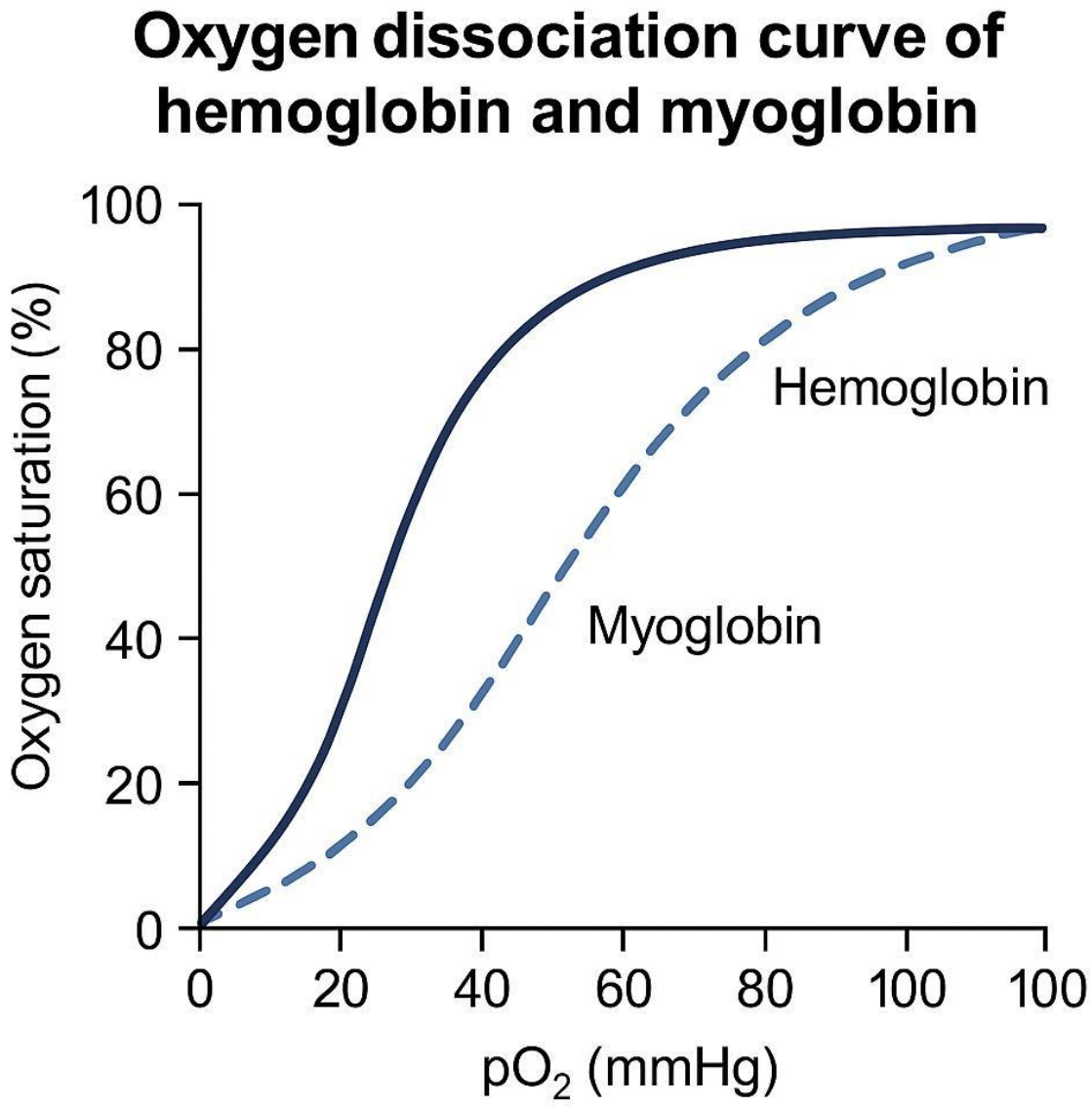

Figure II.2. Oxygen dissociation curve of hemoglobin (sigmoidal) compared to myoglobin (hyperbolic), illustrating cooperative oxygen binding in hemoglobin.[50]

Additionally, hemoglobin's oxygen affinity is modulated by several physiological factors, including pH (Bohr effect), carbon dioxide levels, temperature, and 2,3-bisphosphoglycerate (2,3-BPG). These interactions ensure adaptive oxygen delivery under varying metabolic conditions.

1.2.3 Hemoglobin Derivatives and Functional States

Hemoglobin exists in multiple functional forms, each with distinct properties:

- Oxyhemoglobin (HbO_2): oxygen-bound form responsible for oxygen transport.
- Deoxyhemoglobin (HHb): the form without oxygen, typically found in venous blood.
- Methemoglobin (MetHb): oxidized form (Fe^{3+}) that cannot bind oxygen effectively.

- Carboxyhemoglobin (COHb): carbon monoxide-bound form, which has much higher affinity than oxygen and is toxic.

The transition between oxyhemoglobin and deoxyhemoglobin is central to its physiological role. The deoxygenated form (HHb), of particular interest in this study, can participate in redox reactions and is more susceptible to aggregation or oxidative modifications under stress conditions.[51]

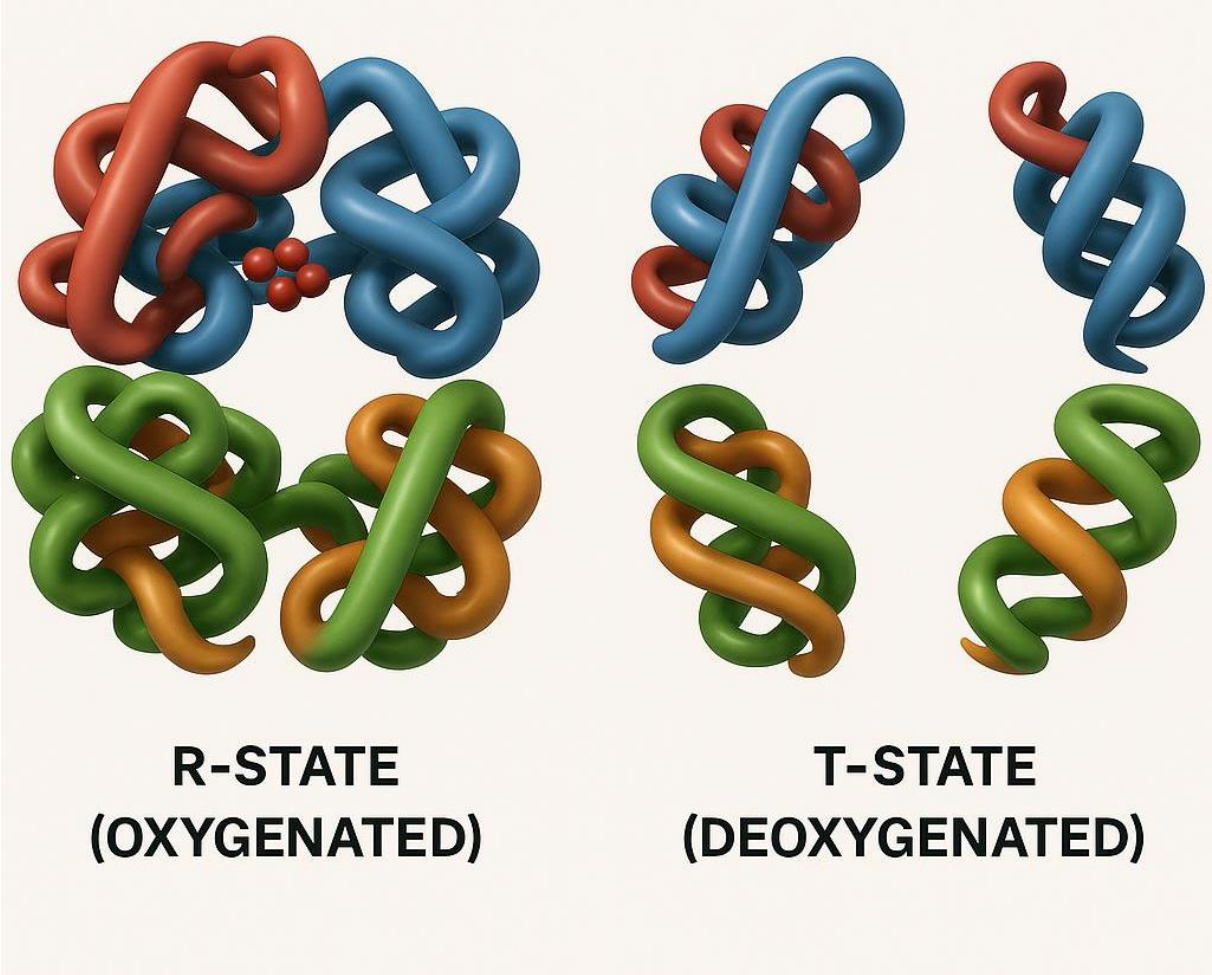

Figure II.3. Structural comparison between oxyhemoglobin and deoxyhemoglobin forms. The R-state (oxygenated) and T-state (deoxygenated) exhibit distinct quaternary conformations.[52]

1.2.4 Hemoglobin and Redox Activity

Beyond oxygen transport, hemoglobin contributes to redox homeostasis and nitric oxide (NO) signaling. However, free hemoglobin released during hemolysis can promote oxidative damage through Fenton-like reactions involving ferrous (Fe^{2+}) and ferric (Fe^{3+}) iron. The heme moiety itself can intercalate into lipid membranes and catalyze lipid peroxidation, exacerbating cellular injury.[53]

Under pathological conditions, the accumulation of deoxyhemoglobin and heme can trigger pro-inflammatory responses and cytotoxic effects. Therefore, monitoring the oxidative status and structural integrity of hemoglobin is essential in understanding the cytotoxic potential of interacting compounds.

1.3 Hemoglobin Derivatives and Their Biological Relevance

Hemoglobin (Hb) exists in multiple chemical forms, depending on its ligands and oxidation state. These derivatives play vital roles in both physiological and pathological contexts. Changes in the hemoglobin structure or redox state can impact oxygen transport capacity, red blood cell lifespan, and overall cellular homeostasis. Among these derivatives, **deoxyhemoglobin (HHb)** is of particular interest due to its involvement in oxygen release, redox activity, and susceptibility to oxidative modification.[54]

1.3.1 Deoxygenated Hemoglobin (HHb): Structure and Significance

Deoxyhemoglobin (HHb) represents the form of hemoglobin in which all four heme iron centers are in the **ferrous (Fe^{2+})** state but **not bound to oxygen**. This form is predominantly found in venous blood and is responsible for transporting carbon dioxide back to the lungs. Structurally, HHb adopts the **tense (T) state**, characterized by a lower affinity for oxygen and a more compact quaternary conformation compared to oxyhemoglobin (R state).[55]

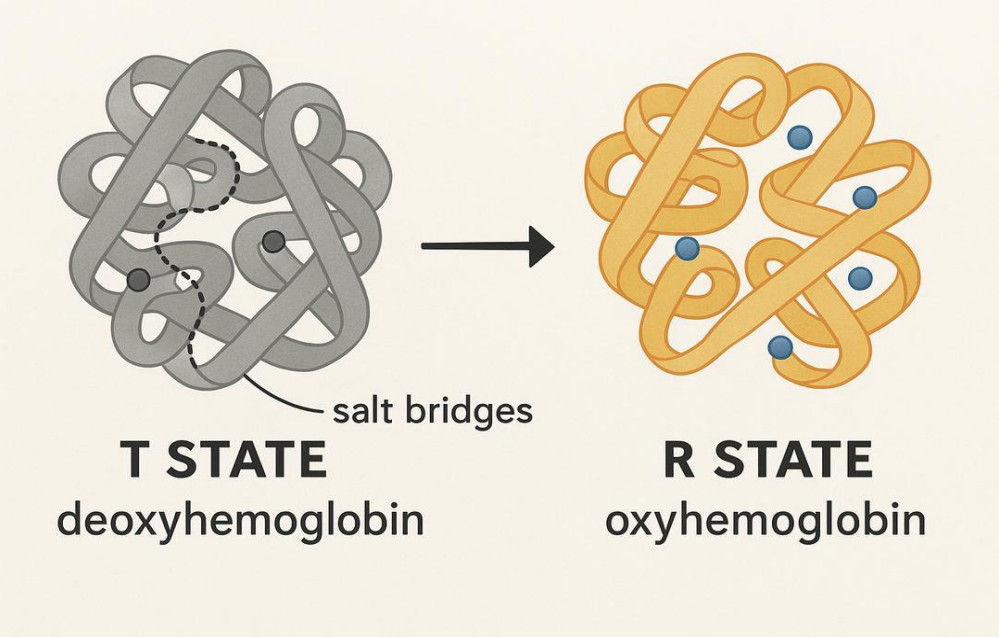

Figure II.4. Transition between the T (tense) state of deoxyhemoglobin and the R (relaxed) state of oxyhemoglobin. The T state is stabilized in the absence of bound oxygen.[56]

The stabilization of the T state involves multiple salt bridges and hydrogen bonds, making it energetically less favorable for oxygen to bind. However, once one oxygen molecule binds,

this network is disrupted, shifting the equilibrium toward the R state and facilitating additional oxygen binding—a hallmark of allosteric regulation.

HHb also acts as a **redox-active species**. In hypoxic conditions or during hemolysis, HHb can participate in **electron transfer reactions** and generate reactive oxygen species (ROS), especially in the presence of exogenous agents or transition metals. The presence of HHb in the extracellular environment, such as during hemolysis, can lead to pro-oxidant activity, cell membrane damage, and inflammatory signaling.[57]

1.3.2 HHb in Pathophysiological Conditions

Elevated levels of HHb are commonly observed under hypoxic, ischemic, or anemic conditions. In clinical contexts, HHb serves as a **biomarker of tissue oxygenation**, often monitored through near-infrared spectroscopy (NIRS) or pulse oximetry to assess perfusion status.[58]

In hemolytic disorders, the accumulation of HHb in plasma can have several deleterious effects:

- **Scavenging of nitric oxide (NO):** HHb reacts rapidly with NO, reducing its bioavailability and contributing to **vasoconstriction** and **vascular dysfunction**.
- **Induction of oxidative stress:** The unbound iron in HHb can catalyze **Fenton reactions**, producing hydroxyl radicals that damage membranes, proteins, and DNA.
- **Promotion of inflammation:** HHb and its breakdown products can activate **Toll-like receptors (TLRs)**, triggering inflammatory cascades and immune cell activation.

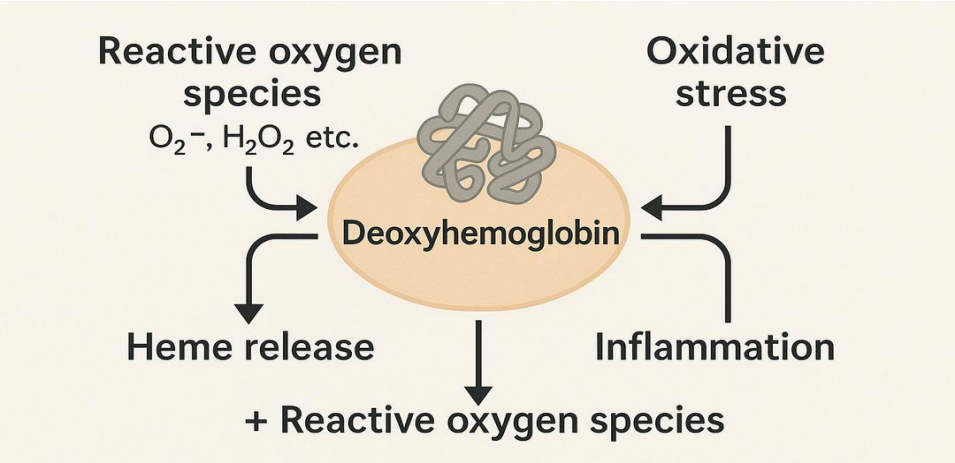

Figure II.5. Overview of deoxyhemoglobin's role in oxidative stress and inflammation. HHb contributes to ROS production, NO scavenging, and activation of pro-inflammatory signaling pathways.[59]

Because of these pathological outcomes, compounds that interact with HHb are of high interest in pharmacological studies, particularly in evaluating potential hemolytic or oxidative toxicity.

1.3.3 Spectroscopic and Electrochemical Properties of HHb

HHb displays distinct spectral characteristics in the visible and near-infrared regions, which make it identifiable and quantifiable via **UV-Vis spectroscopy**. Its Soret band, typically near 430 nm, and Q bands in the 550–580 nm range shift depending on the ligand and redox state of the heme iron.[60]

Electrochemically, HHb exhibits redox behavior associated with the **Fe^{2+}/Fe^{3+} transition**, making it amenable to analysis by cyclic voltammetry and differential pulse voltammetry. These methods are useful for studying drug–Hb interactions and assessing the pro-oxidant or antioxidant potential of test compounds.[61]

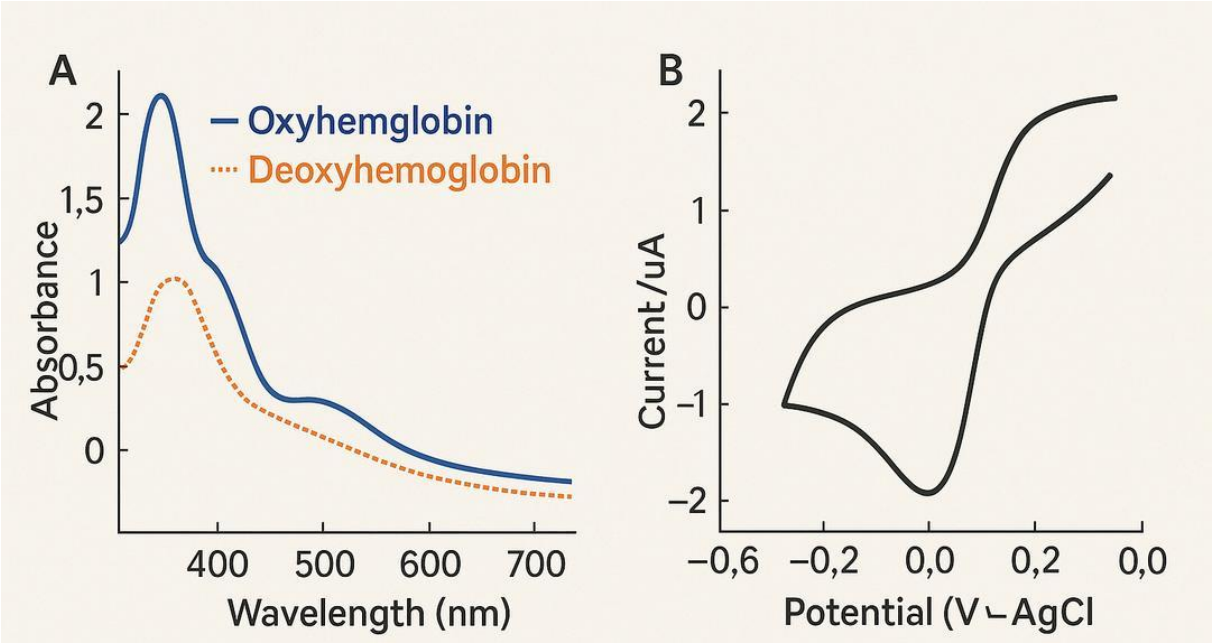

Figure II.6. (A) UV-Vis absorbance spectra of oxyhemoglobin and deoxyhemoglobin. (B) Cyclic voltammogram showing the redox peak of HHb corresponding to Fe^{2+}/Fe^{3+} transition.[62]

In summary, HHb is a functionally significant and redox-sensitive form of hemoglobin that serves as a useful probe for evaluating molecular interactions, especially in the context of hemolysis and oxidative damage. The study of its interaction with synthetic or natural compounds—including porphyrin derivatives—offers insights into the hemolytic potential and redox reactivity of new bioactive agents.

1.4 Hemolysis: Definition and Mechanisms

Hemolysis refers to the destruction or rupture of red blood cells (RBCs), leading to the release of hemoglobin and other intracellular components into the extracellular environment or plasma. Under physiological conditions, red blood cells circulate for about 120 days before being removed by the reticuloendothelial system. However, premature hemolysis can result from chemical, mechanical, infectious, or immune-related factors.[63]

1.4.1 Classification of Hemolysis

Hemolysis can be categorized based on origin or cause into three main types:

- **Intravascular hemolysis:** Occurs within blood vessels, releasing free hemoglobin directly into the bloodstream.
- **Extravascular hemolysis:** Happens in the spleen or liver, where macrophages phagocytize aged or damaged erythrocytes.
- **Chemical or drug-induced hemolysis:** Results from exposure to oxidizing agents, certain drugs, or toxic compounds interacting with RBC membranes or hemoglobin.

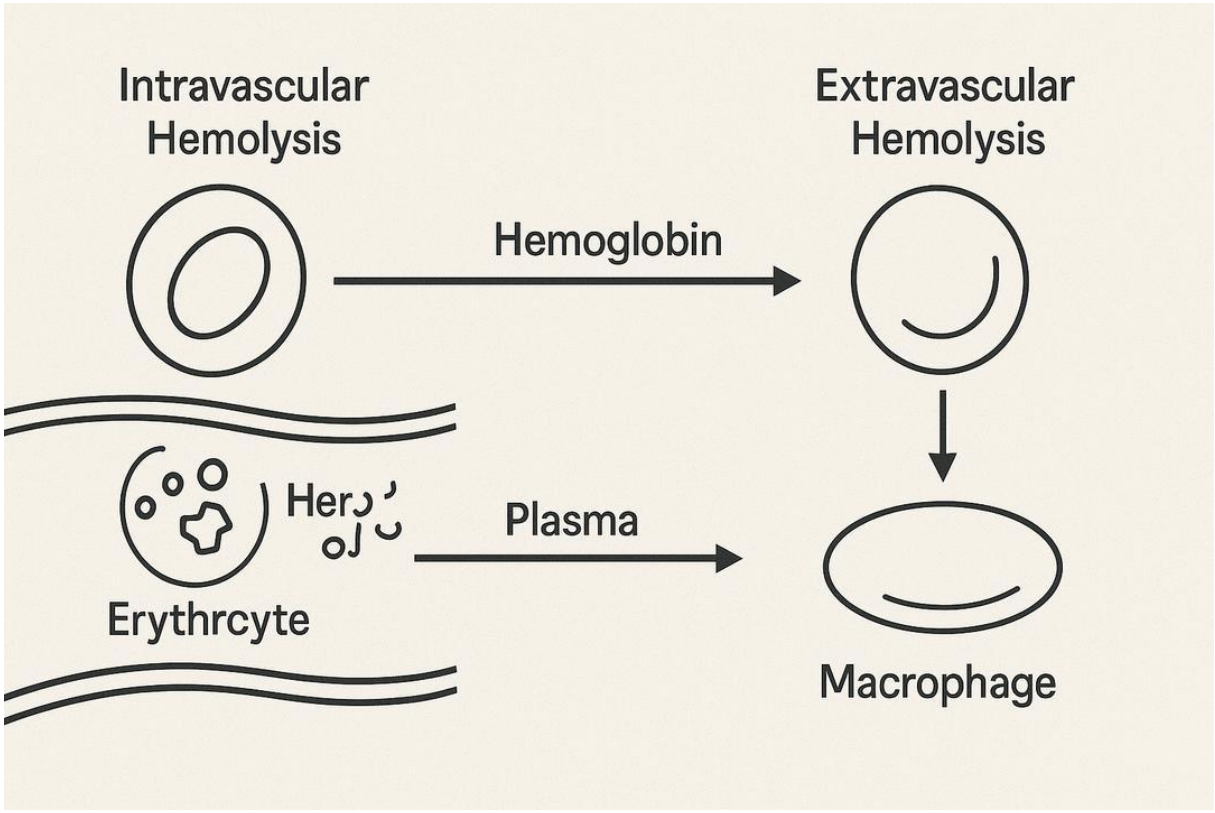

Figure II.7. Schematic representation of intravascular and extravascular hemolysis processes, highlighting the fate of red blood cells and free hemoglobin.[64]

1.4.2 Molecular Mechanisms of Hemolysis

The integrity of the erythrocyte membrane is essential for maintaining cell shape, flexibility, and resistance to mechanical and oxidative stress. Hemolysis occurs when this membrane is compromised due to:

- **Oxidative stress:** Reactive oxygen species (ROS) attack membrane lipids and proteins, leading to lipid peroxidation and loss of membrane stability.
- **Heme toxicity:** Free heme, especially from deoxygenated or oxidized hemoglobin, can intercalate into the lipid bilayer, disrupting structural integrity.
- **Binding of xenobiotics:** Certain compounds bind to membrane proteins or hemoglobin, inducing conformational changes that lead to RBC lysis.
- **ATP depletion or ionic imbalance:** Disruption in Na^+/K^+ pump activity results in cell swelling and rupture.

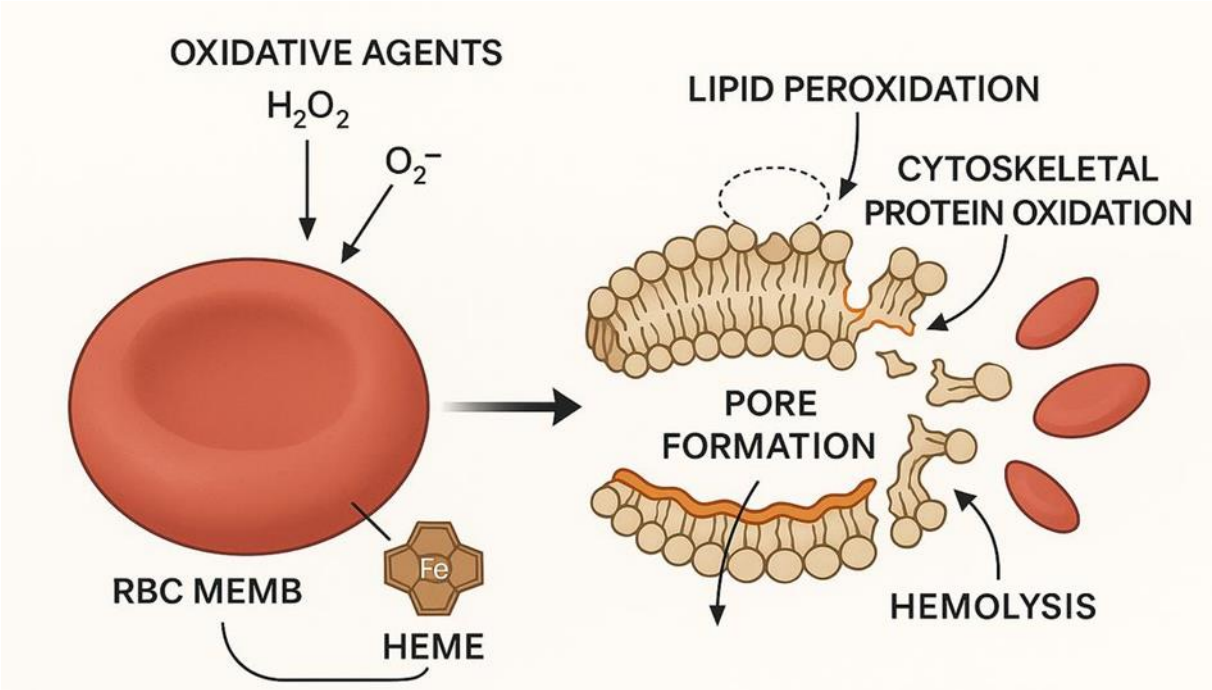

Figure II.8. Illustration of how oxidative agents and heme destabilize the RBC membrane, triggering hemolysis.[65]

1.4.3 Indicators and Detection of Hemolysis

Several biochemical and physical parameters are used to detect and quantify hemolysis:

- **Plasma free hemoglobin (fHb):** Elevated in intravascular hemolysis.
- **Lactate dehydrogenase (LDH):** Released from lysed RBCs.
- **Decreased haptoglobin:** Haptoglobin binds free Hb, so levels drop during hemolysis.

- **Spectrophotometric assays:** Detect absorbance of released hemoglobin in supernatants (commonly at 540–580 nm).
- **Microscopic analysis:** Reveals morphological changes in erythrocytes, including ghost cells and spherocytes.

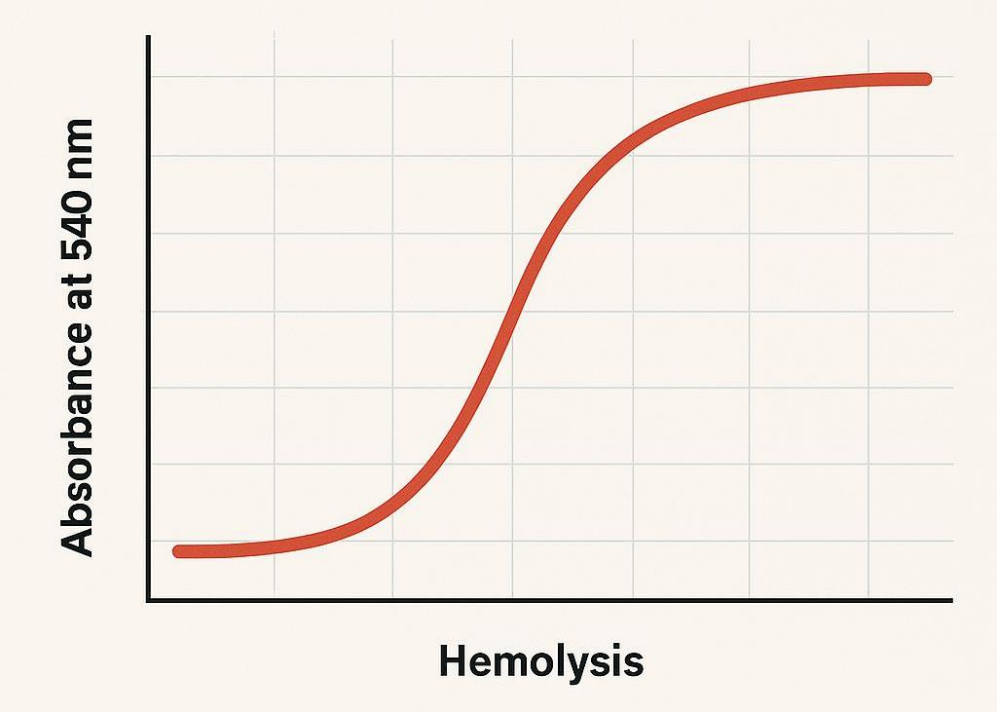

Figure II.9. Absorbance profile indicating the extent of hemolysis through hemoglobin release measured at 540 nm.[66]

1.4.4 Biological Consequences of Hemolysis

Uncontrolled or chronic hemolysis can have several systemic effects:

- **Oxidative injury:** Free heme and iron catalyze the production of ROS, leading to tissue damage.
- **Vascular dysfunction:** Scavenging of nitric oxide by free hemoglobin contributes to vasoconstriction and hypertension.
- **Inflammatory activation:** Hemolysis products activate endothelial cells, leukocytes, and pattern recognition receptors (e.g., TLR4).
- **Renal toxicity:** Hemoglobinuria can cause acute tubular necrosis due to the nephrotoxic effects of heme.

These effects highlight the importance of studying the **hemolytic potential of new compounds**, particularly those interacting with hemoglobin or mimicking heme structures, such as porphyrin derivatives.

1.5 Hemoglobin–Ligand Interactions and Hemolytic Activity of Porphyrinoid Compounds

The interaction of hemoglobin (Hb) with small molecules and ligands significantly influences its structure, stability, and function. Exogenous compounds, particularly those structurally related to heme—such as **porphyrin derivatives**—can affect hemoglobin's conformation, redox state, and membrane interactions. Understanding these interactions is critical when evaluating the hemolytic potential of bioactive or therapeutic compounds.[67]

1.5.1 Nature of Hemoglobin–Ligand Interactions

Hemoglobin interacts with ligands through a variety of mechanisms, including:

- **Covalent or non-covalent binding** to the heme pocket (e.g., O_2, CO, NO, and some drugs).
- **Hydrophobic interactions** between ligands and the globin chains.
- **Electrostatic forces** that stabilize the bound ligand or influence allosteric transitions.

Ligand binding can cause:

- **Structural rearrangements** (T → R state shift),
- **Allosteric regulation** (Bohr effect),
- **Modulation of redox potential** (Fe^{2+}/Fe^{3+} transitions).

(Insert Figure 10 here: Diagram showing the ligand binding sites on hemoglobin, including heme and globin regions)

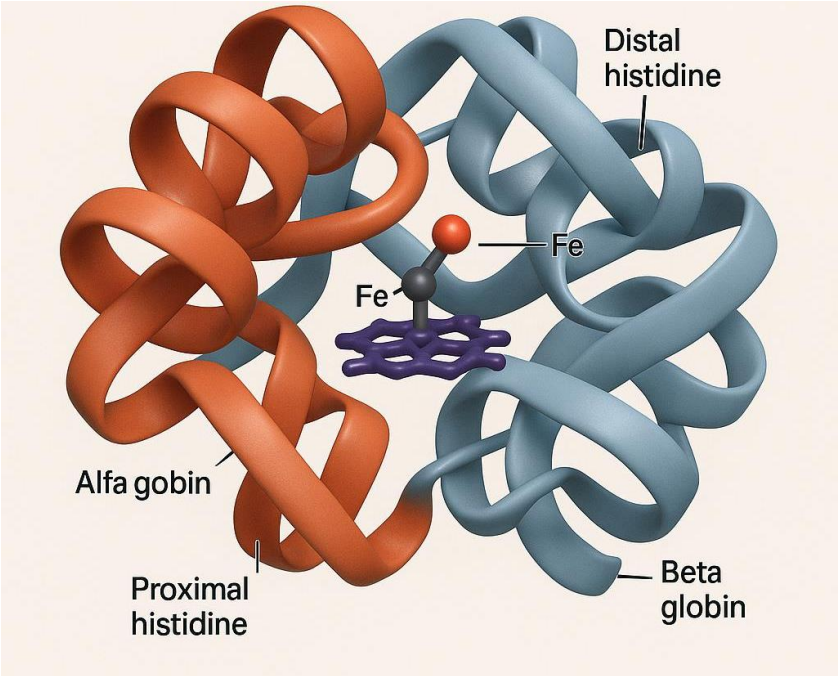

Figure II.10. Structural overview of hemoglobin illustrating the primary ligand interaction sites within the heme pocket and surrounding globin chains.[68]

1.5.2 Porphyrinoid Compounds and Hemoglobin Interaction

Porphyrinoids—including natural porphyrins, synthetic porphyrin derivatives, and metalloporphyrins—share structural similarity with the heme group and are known to interact with biological systems, especially proteins involved in redox reactions. Their **planar aromatic macrocycle** allows stacking or intercalation with biomolecules, and the central metal ion (when present) can mimic or disrupt the iron center of heme.[69]

These compounds may:

- Compete with oxygen for heme binding.
- Displace or alter the oxidation state of iron in hemoglobin.
- Insert into lipid bilayers of RBC membranes, indirectly affecting hemoglobin conformation.
- Trigger oxidative reactions, especially if the porphyrinoid is redox-active.

(Insert Figure 11 here: Structural comparison between heme and synthetic porphyrin derivatives)

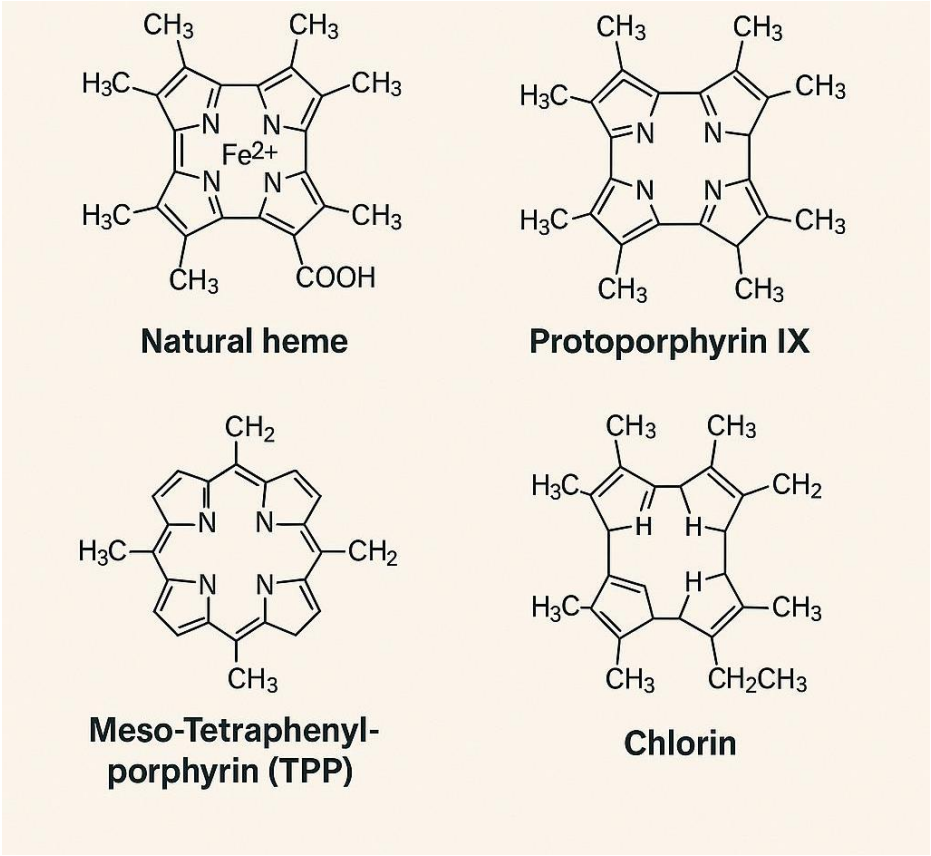

Figure II.11. Chemical structures of natural heme and representative porphyrinoid derivatives used in biological studies.[70]

1.5.3 Hemolytic Activity of Porphyrin Derivatives

Porphyrinoid compounds are double-edged swords: while they offer therapeutic promise in photodynamic therapy, antimicrobial, or anticancer applications, some can induce **hemolytic toxicity**.[71] Mechanisms include:

- **Oxidative damage to RBC membranes:** Metalloporphyrins can generate singlet oxygen or ROS upon light activation or redox cycling.
- **Direct interaction with hemoglobin:** Resulting in denaturation, oxidation to methemoglobin, or heme displacement.
- **Membrane disruption:** Due to their lipophilic character, some porphyrins integrate into lipid bilayers, altering fluidity and permeability.

(Insert Figure 12 here: Illustration of how porphyrin derivatives interact with RBCs and induce hemolysis)

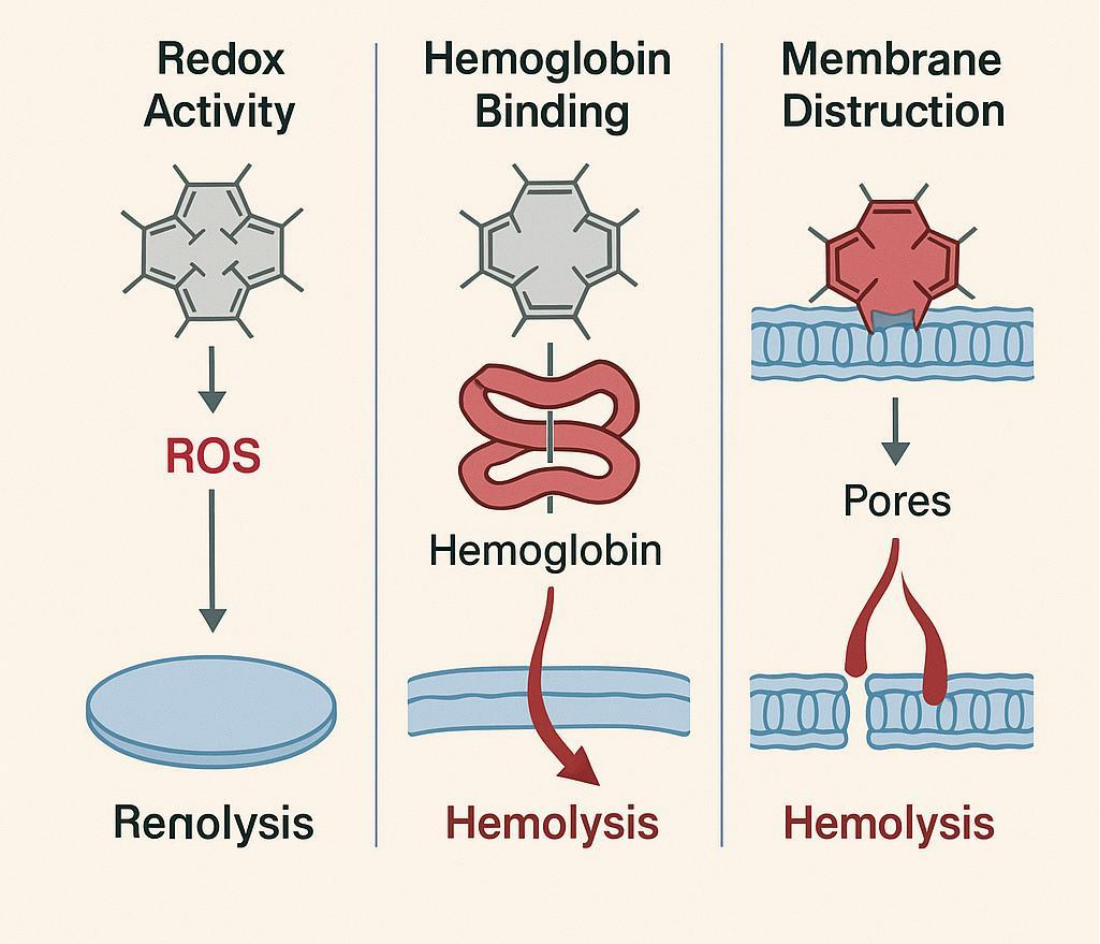

Figure II.12. Proposed mechanisms of porphyrin-induced hemolysis, involving redox activity, hemoglobin binding, and membrane disruption.[72]

Several studies have confirmed these effects:

- **In vitro assays** using spectrophotometric or electrochemical methods show increased hemoglobin oxidation and membrane leakage.
- **Hemolysis assays** reveal concentration-dependent RBC rupture upon porphyrin exposure.
- **Molecular docking and dynamics** simulations support direct binding of porphyrinoids to the heme center or globin chains, influencing protein dynamics.

1.5.4 Implications for Biomedical Applications

While porphyrinoids hold great pharmacological potential, their hemolytic side effects must be carefully evaluated. Modifications in side chains, metal centers, and overall lipophilicity can reduce toxicity and improve selectivity. Therefore, studies involving these compounds must balance efficacy with biocompatibility.

This justifies the need for **comprehensive in vitro, in silico, and in vivo evaluations** of newly synthesized porphyrin derivatives, particularly focusing on their interactions with HHb and their hemolytic behavior. [73]

Second part

Experimental

Chapter I

Materials & methods

1. Chemicals and reagents:

- Dimethylformamide (DMF) (analytical grade from PROLABO) was used as a solvent in the biological tests.
- 2,2-diphenyl-1-picrylhydrazyl (DPPH) (99 %), from Alfa Aesar;
- α-tocopherol ($C_{29}H_{50}O_2$, MW = 430.71) (97%), from Alfa Aesar;

2. UV-Vis Absorption Spectroscopy for Hemoglobin–Ligand Interaction and Hemolysis Evaluation

Ultraviolet-visible (UV-Vis) absorption spectroscopy is a fundamental analytical technique widely employed in biochemical studies to investigate ligand–protein interactions and evaluate structural changes or stability of biomacromolecules. In the context of hemoglobin (HHb), this technique provides valuable insight into conformational modifications, oxidation states, and potential denaturation upon exposure to external agents such as porphyrin derivatives.[74]

UV-Vis spectroscopy operates within the wavelength range of 200–800 nm, encompassing both ultraviolet (UV: 200–400 nm) and visible (Vis: 400–800 nm) regions. When hemoglobin interacts with exogenous compounds, characteristic spectral changes—such as shifts in the Soret band (~410 nm) and alterations in the Q-bands (~540 and ~576 nm)—can indicate binding events, heme distortion, or oxidation (e.g., conversion from Fe^{2+} to Fe^{3+}).

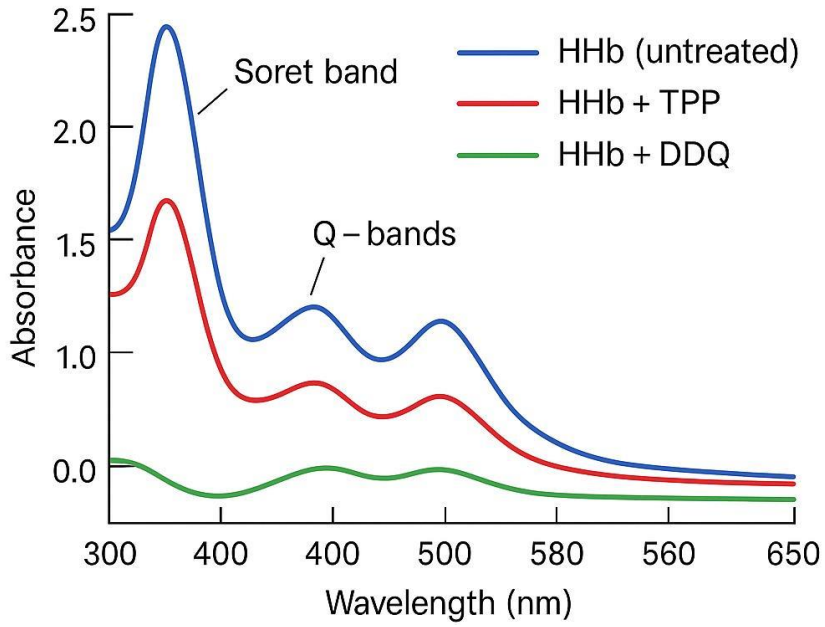

Figure I.1: UV-Vis spectra of human hemoglobin (HHb) before and after incubation with porphyrin ligands, illustrating characteristic hypochromic and bathochromic effects.[75]

In addition, UV-Vis measurements are essential for assessing hemolysis, a process in which red blood cells (RBCs) rupture and release hemoglobin into the extracellular medium. This is typically monitored by measuring the absorbance of the supernatant at 414 nm (Soret band) after centrifugation. An increase in absorbance correlates with elevated levels of free hemoglobin in solution, thereby quantifying the extent of hemolysis.

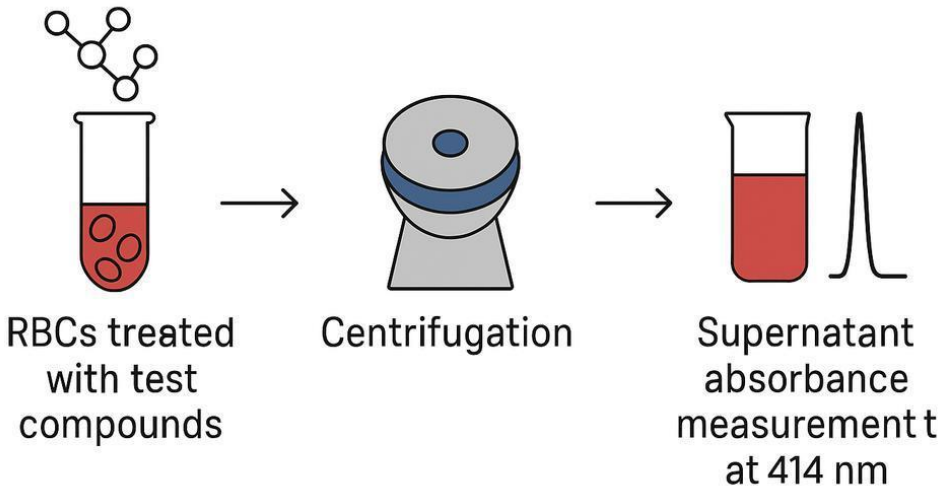

Figure I.2. Workflow for hemolysis evaluation using UV-Vis spectroscopy: RBCs treated with test compounds → centrifugation → supernatant absorbance measurement at 414 nm.[76]

The strength of the interaction between porphyrin ligands and hemoglobin can also be quantified through binding constant (K_b) calculations, based on changes in absorbance upon titration of the ligand with HHb. The Benesi-Hildebrand equation (Equation II.8) is adapted for such systems:

$$\frac{A_0}{(A - A_0)} = \frac{\varepsilon_G}{\varepsilon_{H-G} - \varepsilon_G} + \frac{\varepsilon_G}{\varepsilon_{H-G} - \varepsilon_G} \frac{1}{K_b[HHb\,]} \quad (II.8)$$

Where:

- *[HHb]* is the concentration of hemoglobin,
- K_b is the intrinsic binding constant,
- A_0 and A are the ligand's absorbance in the absence and presence of HHb,
- ε_G and ε_HG are the molar extinction coefficients of the free and bound forms, respectively.

Plotting $A_0/(A-A_0)$ versus 1/[HHb] yields a linear relationship from which K_b can be derived (slope/intercept). A binding constant in the range of 10^4 to 10^6 M^{-1} suggests strong and specific interaction, which could influence hemoglobin stability and redox behavior.[77]

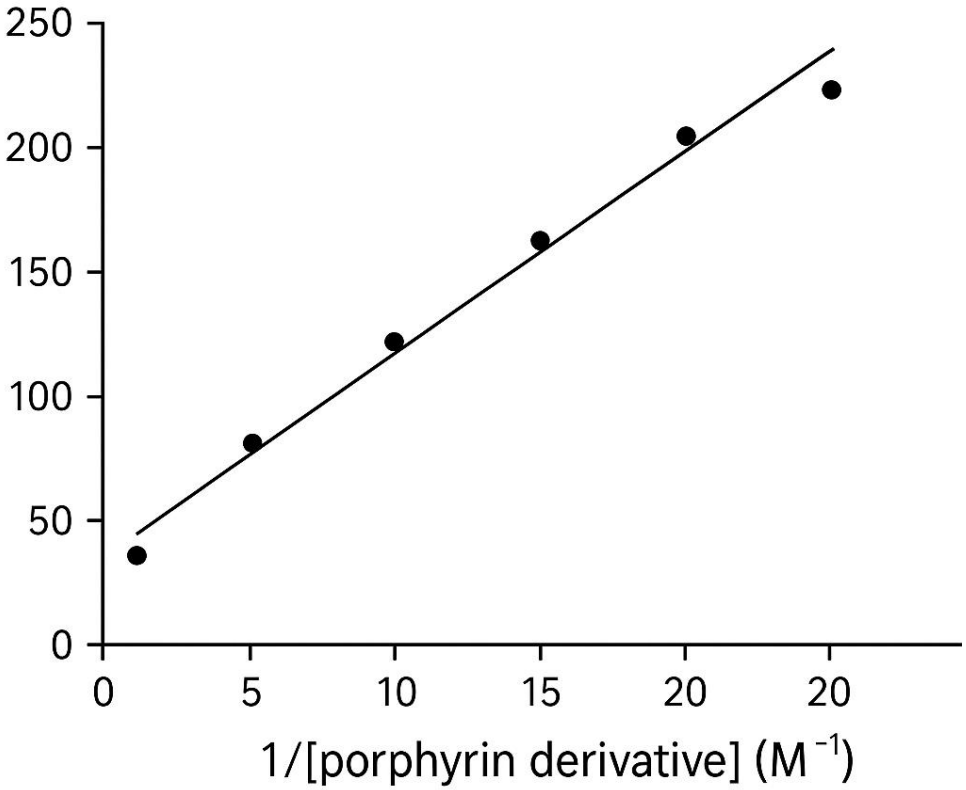

Figure I.3. Linear Benesi-Hildebrand plot for determining the binding constant (K_b) between porphyrin derivative and HHb. [78]

This UV-Vis-based approach thus serves a dual purpose: elucidating hemoglobin–ligand interactions and evaluating the hemolytic potential of tested compounds, contributing to the early-phase screening of bioactive molecules in medicinal chemistry and toxicology studies.

3. UV-Visible Measurements:

UV-Vis spectroscopic investigations were carried out using a Shimadzu UV-1800 spectrophotometer equipped with a quartz cell of 5 mL capacity. All measurements were conducted at room temperature (25 ± 1 °C). Data acquisition was performed using UV Probe software version 2.34, and subsequent graphical analysis and curve fitting were completed with OriginLab version 2.0 (Integral Software, France).[79]

The porphyrin derivatives were first characterized by acquiring their absorption spectra in 1 mM DMF solutions to determine their intrinsic electronic transitions, including the Soret and Q bands, prior to interaction studies.

To assess the interaction with hemoglobin (HHb), a fixed concentration of each porphyrin derivative (typically 1 mM) was titrated with increasing concentrations of HHb in phosphate-buffered saline (PBS, pH 7.4). After each addition, the absorption spectrum was recorded in the 200–700 nm range. Notable spectral changes—such as hypochromism, bathochromic or hyperchromic shifts in the Soret band (around 410 nm)—were monitored to evaluate binding strength and complex formation.[80]

In the hemolysis assay, UV-Vis spectroscopy was used to quantify the extent of red blood cell lysis. Red blood cells (RBCs) were incubated with different concentrations of the porphyrin derivatives for 1 hour at 37 °C. After incubation, samples were centrifuged at 3000 rpm for 10 minutes, and the absorbance of the supernatant was measured at 414 nm, corresponding to the release of hemoglobin. The degree of hemolysis was calculated by comparing the absorbance with that of the positive control (100% hemolysis with distilled water) and the negative control (PBS only).[81]

Figure I.4. Schematic representation of the UV-Vis-based hemolysis evaluation protocol.[82]

This dual-purpose UV-Vis protocol enables the simultaneous assessment of both hemoglobin–ligand binding behavior and the cytotoxic potential of the tested compounds via membrane disruption, making it a robust screening method in the early stages of bioactivity profiling.

4. Molecular docking

Molecular docking is a widely utilized computational, structure-based approach in pharmaceutical research and drug discovery. It allows for the elucidation of interactions between a ligand, usually a small molecule, and a receptor, typically a macromolecule, as well as the calculation of their binding energy. Moreover, it provides insights into identifying the most suitable candidate ligand for optimal interaction with a designated target receptor.

Molecular docking mainly consists of two stages: an engine for sampling conformations/orientations and a scoring function, which associates a score with each predicted pose.

Molecular docking involves predicting the optimal conformation between two molecules to form a stable complex (see Figure 1.24). This method allows for the discovery of new molecules

through the assembly of two or more molecules, or for gaining insights into the nature of a molecular complex through crystallography

Various experimental techniques, including cyclic voltammetry and electron spectroscopy, typically facilitate the investigation of receptor-ligand interactions and the assessment of binding energy. However, to delve into the specifics of these interactions, predictive simulation methods serve to complement and enhance these experimental approaches [83].

Molecular docking simulation is the most widely used predictive approach in the field of medical and pharmaceutical research.

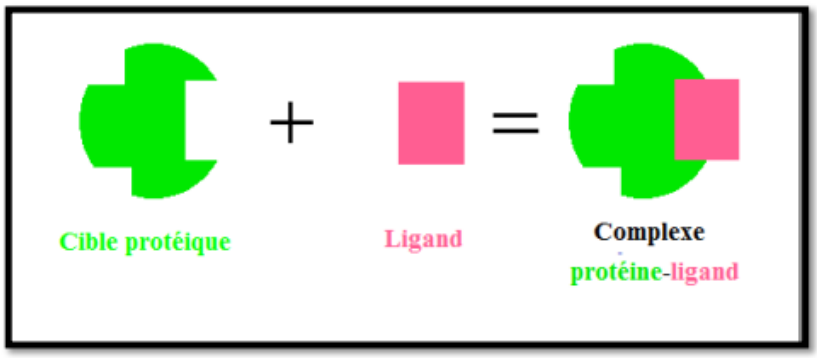

Figure I.5. Schematic representation of the docking of two molecules[84]

4.1.Different types of molecular docking:

Widely used docking software tools employ various search algorithms, including genetic algorithms, fragment-based algorithms, Monte Carlo algorithms, and molecular dynamics algorithms. Additionally, specific tools such as DOCK, GOLD, FlexX, and ICM are primarily utilized for high-throughput docking simulations. Different molecular docking procedures are employed depending on whether ligand/target flexibility is considered or if rigidity is maintained, based on the objectives of the docking simulations.[85] Specifically, these procedures may include:

- ✓ Flexible ligand docking, which involves incorporating the target as a rigid molecule. This is the most commonly used method in docking.
- ✓ Rigid docking, where both the target and ligand molecules are kept rigid.
- ✓ Flexible docking involves both interacting molecules as flexible.

4.2. AutoDock molecular docking software:

Within this software framework, the docking procedure relies on trajectory simulations, characterized by a higher degree of precision compared to starting from an arbitrary position outside the active site. The ligand systematically explores the designated site through iterative

sequences of movements and assessments of ligand-receptor interactions. These movements include translational, rotational, and conformational changes. The interaction energy is quantified using an energy function.

The movements of each subsequent cycle are guided by the energy variations induced by the movements of previous cycles. The algorithm terminates when it identifies the optimal ligand position in the receptor. These techniques better account for the flexibility of the ligand and facilitate the exploration of larger regions.

4.3. Molecular modeling:

In the broader conceptual domain, the term 'modeling' refers to a relatively streamlined portrayal of a procedural phenomenon. Molecular modeling, as implied by its name, occurs within chemical and/or biological contexts to simulate such systems and predict specific properties of interest. To achieve this, molecular modeling relies on mathematical formalisms, which vary in their proximity to physical reality, with quantum chemistry and molecular mechanics (MM) being the two main approaches.

Understanding the atomic-level mechanisms behind interactions between ions and mineral surfaces is crucial. Predominantly utilized simulation techniques include molecular dynamics (MD), the Monte Carlo method, and geometry optimization [86]. These methodologies involve determining equilibrium structures and the energetic characteristics of sorbed species through computations of interatomic interaction energies, guided by the principles of statistical mechanics .

Inter atomic energies are calculated either directly using quantum mechanical methods or by employing empirical interaction parameters, which are calibrated based on quantum mechanical calculations or experimental data for simplified model systems. The primary limitations of molecular mechanics (MM) simulations are associated with the size of the system and the timescale that can be considered in the modeling process.[87]

4.4. Modelling of the energy potential:

To calculate the free energy of the ligand-receptor complex, AutoDock integrates conventional force field terms and supplements them with two entropy-related components.

The following equation expresses the energy:

$$\mathbf{\Delta G} = \Delta G_{vdw} + \Delta G_{hbond} + \Delta G_{elec} + \Delta G_{tor} + \Delta G_{sol} \qquad \text{II.9}$$

ΔG_{vdw}: represents the energy of dispersion/repulsion of atoms,

ΔG_{hbond}: represents the energy of the hydrogen bonds,

ΔG_{elec}: represents the energy of electrostatic interactions,

ΔG_{tor}, is a term that expresses the increase of energy of the system due to the restriction of the free rotors of the ligand and to the restriction of the rotations and translations of the ligand during the complexation with the receptor,

ΔG_{sol}:is an additional nomenclature about entropy,

which characterizes alterations in system energy when the ligand undergoes desolation upon forming a complex with the receptor..

The transition via a QSAR-type empirical relationships essential to establish a connection between the structure of the complexes and the free energy of bonding. Within AutoDock, the utilized empirical model adopts the form of a multiple linear regression incorporating various terms derived from the free energy equation. Eachtermis accordingly weighted by a coefficient obtained from a comprehensive dataset of receptor-inhibitor complexes with known inhibition constants, Ki. Equation II.9 delineates the relationship between the inhibition constant and the free bond energy.

$$\Delta G = RT \ln K_i \qquad \text{(II.10)}$$

Where R is the perfect gas constant;

T is the absolute temperature

4.5. The Force Field:

In the domain of theoretical chemistry, the force field represents the potential energy of a deformable molecule or a set of interacting molecules, without directly involving quantum mechanics. It describes the potential energy according to a mathematical expression, as a function of the deformation coordinates of the molecules and the intermolecular distances, and is dependent on characteristic parameters of the interaction forces between atoms.[88]

To determine the optimal arrangement of a group of atoms, it is necessary to reduce the three Cartesian coordinates per atom (resulting in 3000 Cartesian coordinates for a protein comprising 1000 atoms). Consequently, we must find the minimum of a function (energy) in a space of a few thousand variables. Thus, the challenge lies in selecting a potential function of analytical simplicity capable of accurately representing these molecular coordinates. This function must be simple enough to calculate quickly and yet sufficiently precise to simulate the structural and thermodynamic properties of macromolecules acceptably. Comprising various potential energy functions, a force field delineates the intramolecular interactions among both bonded and non-bonded atoms.

$$E_{Total} = E_{stretch} + E_{bend} + E_{tors} + E_{vanderwalls} + E_{électro} + \cdots \qquad \text{II. 11}$$

One of the primary challenges in molecular modeling (MM) is the selection of suitable parameters to model the molecular system under investigation. The distinctive features of each force field are determined by the number of constituents terms within the overarching equation, a quantity that typically increases with the complexity of the force field.[89]

4.6. The theory of the functional density (DFT):

The Density Functional Theory (DFT) is a theory (in principle exact) of electronic structure based on the distribution of electronic density n(r), instead of the multi-electron wave function Ψ(r1, r2, r3, ...). Widely used for over 30 years by physicists working on the electronic structure of solids, surfaces, defects, etc., it has also recently become popular among theoreticians and computational chemists. This article is addressed to the chemical community. It aims to convey the basic concepts and the breadth of applications: the current state and trends of approximation methods (local density and generalized gradient approximations, hybrid methods) and the new insights that DFT has provided on important concepts such as electronegativity, hardness, and the chemical reactivity index.[90]

Chapter II

Results & discussion

1. Molecular Docking of Porphyrins with HHb

A molecular docking study was performed on the synthesized porphyrin derivatives $NiTPPH_2$, $TbiPPH_2$, $TPPH_2$ (o-methyl), and $ZnTPPH_2$ (p-methyl) to predict their potential binding modes with human hemoglobin (HHb) and to visualize their interactions within the protein structure. These simulations allowed the identification of the preferred binding sites and the optimal orientation of each ligand within the HHb active or allosteric regions.

1.1. Structural Optimization

Prior to docking, the three-dimensional structures of the four porphyrin ligands were fully optimized using density functional theory (DFT) without imposing any symmetry constraints. All calculations were performed using the Gaussian 09 software package .[93] The hybrid functional B3LYP, combining Becke's exchange functional and the Lee–Yang–Parr correlation functional, was used in conjunction with the LanL2DZ basis set, suitable for transition metal-containing complexes .[94] The optimized molecular geometries are presented in Figure I.6.

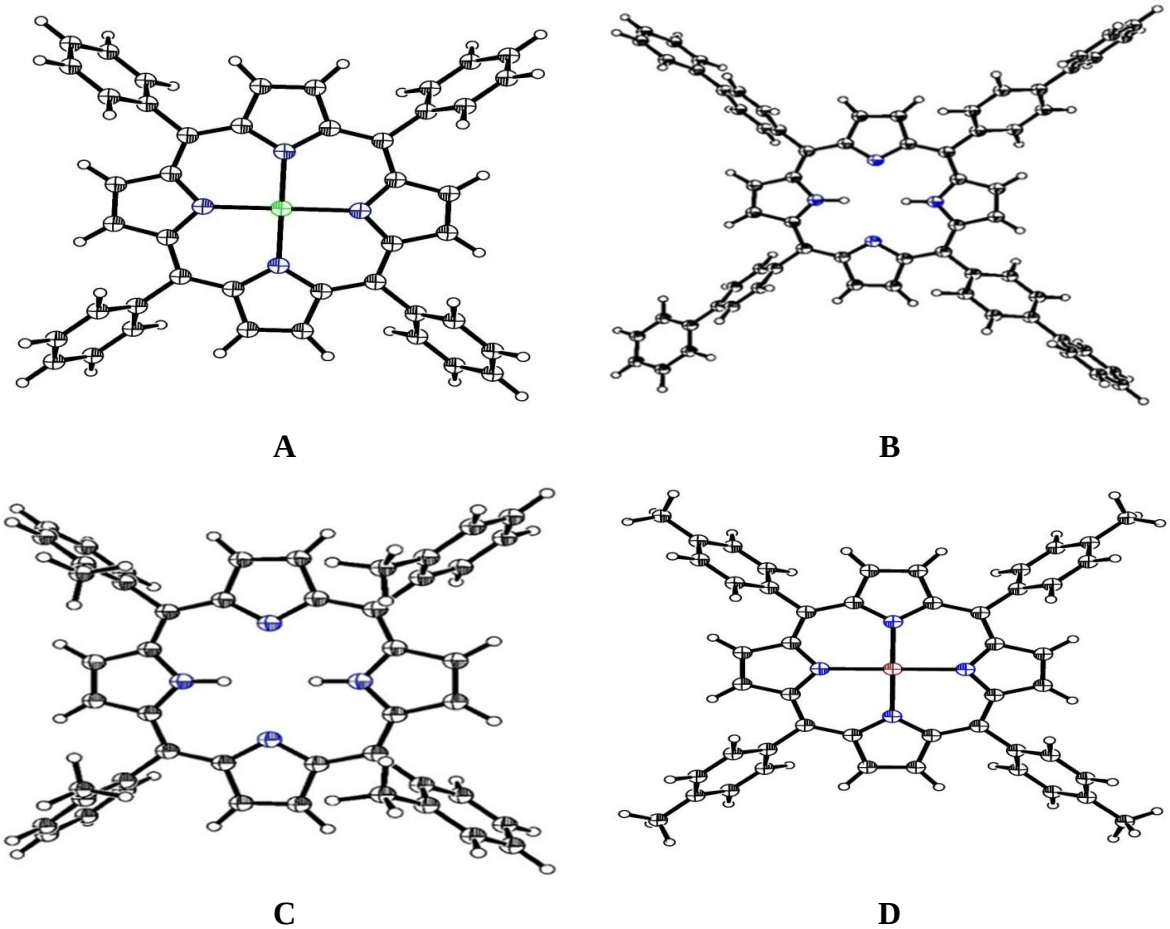

Figure I.6. 3D conformation of ligands: $NiTPPH_2$ (A), $TbiPPH_2$ (B), $TPPH_2$(o-methyl) (C), and $ZnTPPH_2$ (p-methyl) (D), (ORTEP View 03, V1.08);thermal ellipsoids are plotted at the 50% probability level

1.2 Docking simulations:

Molecular docking studies of the ligands with human hemoglobin (HHb) were carried out using AutoDock 4.2 software. The optimized structures of each porphyrin ligand and the HHb protein were prepared and imported into the AutoDock environment. All torsional bonds in the ligands were set as flexible, while the HHb structure was kept rigid during the simulation.

The docking simulations were performed on a Pentium 2.20 GHz microcomputer with 4.00 GB of RAM, operating under Windows 10. Grid maps were generated using AutoGrid, centered on the active region of the HHb molecule with appropriate dimensions to accommodate the ligands. The Lamarckian Genetic Algorithm (LGA) was applied to search for the most favorable binding conformations. Each docking run consisted of 100 GA runs with default parameters.

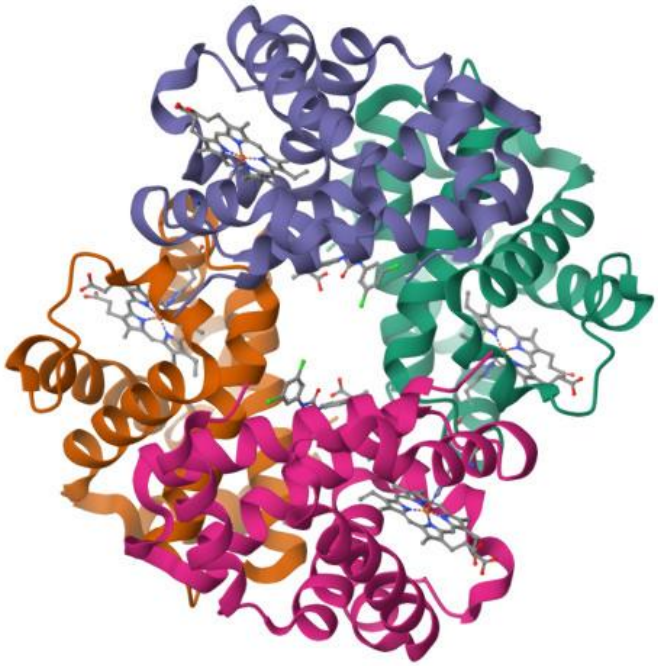

Figure I.7. Crystal structure of HHb (PDB ID: 2D60).

The hemoglobin structure (PDB ID: 2D60) was retrieved from the Protein Data Bank (http://www.pdb.org) and used as the receptor to investigate the binding interactions with the synthesized porphyrin ligands. Prior to docking, the HHb structure was preprocessed by removing crystallographic water molecules and any non-receptor molecules. Hydrogen atoms were subsequently added, and Kollman charges were assigned to the protein using AutoDock Tools.

The molecular docking calculations were conducted using the Lamarckian Genetic Algorithm (LGA). A grid box of 60 × 60 × 60 Å was defined with a grid spacing of 0.375 Å,

centered at coordinates X = 2.994, Y = -1.474, Z = 10.745. The docking protocol consisted of 50 runs, each with 250,000 energy evaluations, while all other parameters were maintained at their default settings.

The most favorable conformation for each ligand–HHb complex was selected based on the lowest binding energy. The calculated binding affinities of $NiTPPH_2$, $TbiPPH_2$, $TPPH_2$ (o-methyl), and $ZnTPPH_2$ (p-methyl) with hemoglobin are reported in Table II.4.

Table II.4. Binding constant and binding free energy values obtained for HHb–$NiTPPH_2$, HHb–$TbiPPH_2$, HHb–$TPPH_2$ (o-methyl), and HHb–$ZnTPPH_2$ (p-methyl) adducts by molecular docking approach

Adduct	**K (M^{-1})**	**$-\Delta G$ ($kJ \cdot mol^{-1}$)**
HHb – $NiTPPH_2$	3.11×10^5	31.12
HHb – $TbiPPH_2$	1.88×10^5	29.04
HHb – $TPPH_2$ (o-methyl)	1.02×10^5	27.10
HHb – $ZnTPPH_2$ (p-methyl)	6.53×10^4	26.06

The results indicate that $NiTPPH_2$ exhibits the highest binding affinity towards hemoglobin, followed by $TbiPPH_2$ and $TPPH_2$ (o-methyl), while $ZnTPPH_2$ (p-methyl) shows the weakest binding.

Moreover, the molecular docking simulations suggest that all four ligands form stable interactions with HHb, although no hydrogen bonds were detected between the ligands and the hemoglobin amino acid residues. The interactions are predominantly electrostatic or hydrophobic in nature, suggesting that the porphyrin macrocycles favor non-covalent stabilization within the HHb binding pocket.

The interaction modes of each ligand with HHb are illustrated in the figure below.

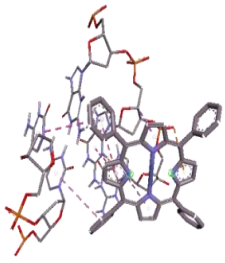

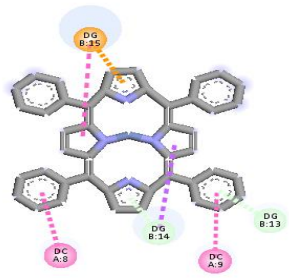

$NiTPPH_2$

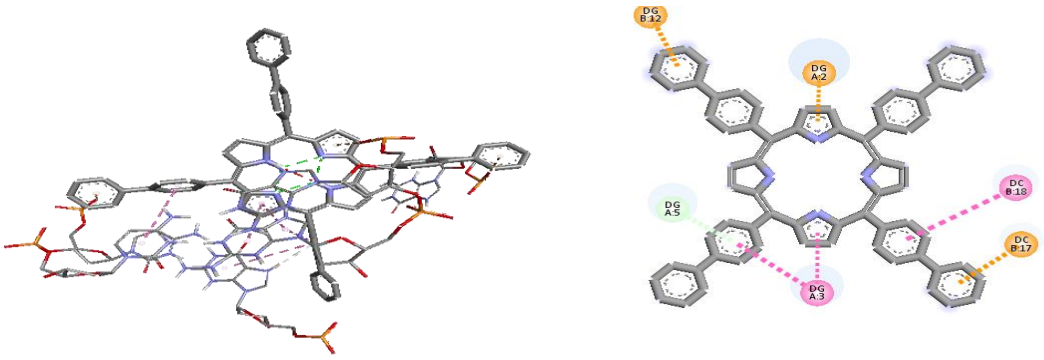

TbiPPH$_2$

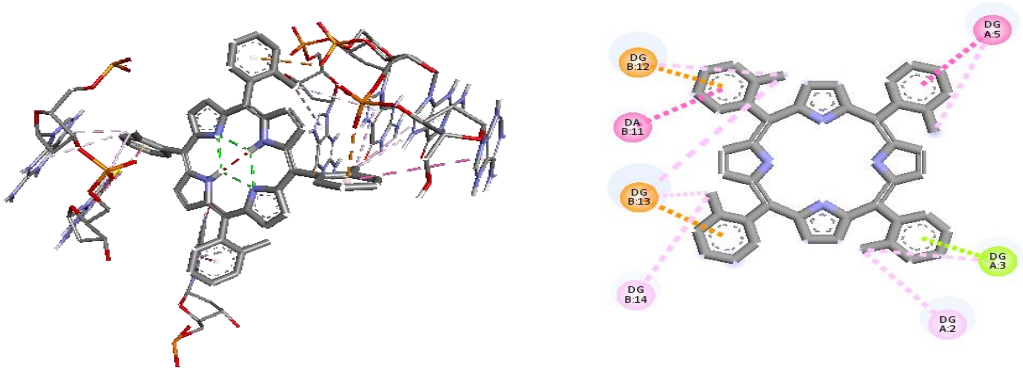

TPPH$_2$ (o-methyl)

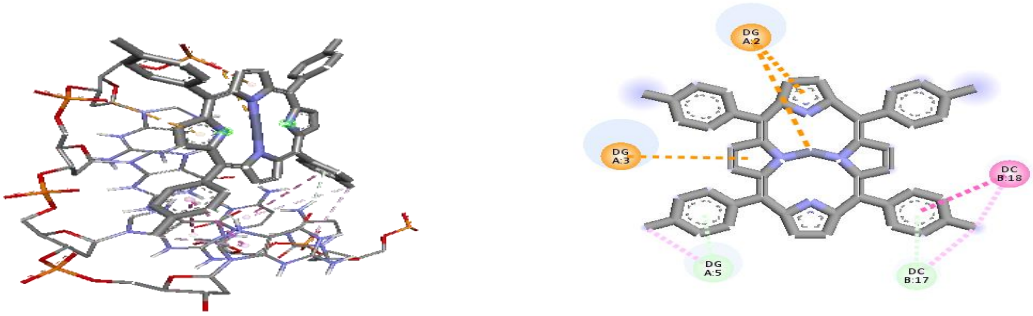

ZnTPPH$_2$ (p-methyl)

Figure.I.8. 2D and 3D presentation of the porphyrin derivatives ligands with the HHb

2. Chemical Product:

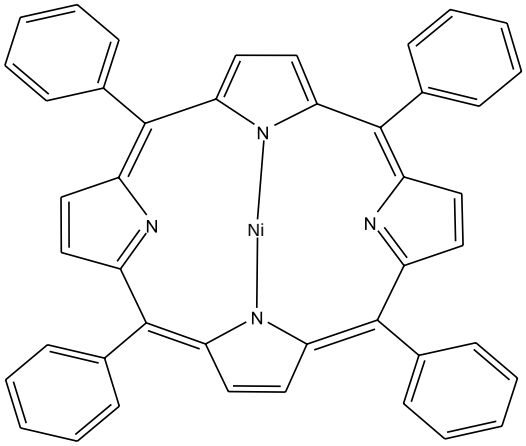

P1 : Nikel tetraphenyl-porphyrin

$NiTPPH_2$ ($C_{44}H_{28}N_4Ni$)

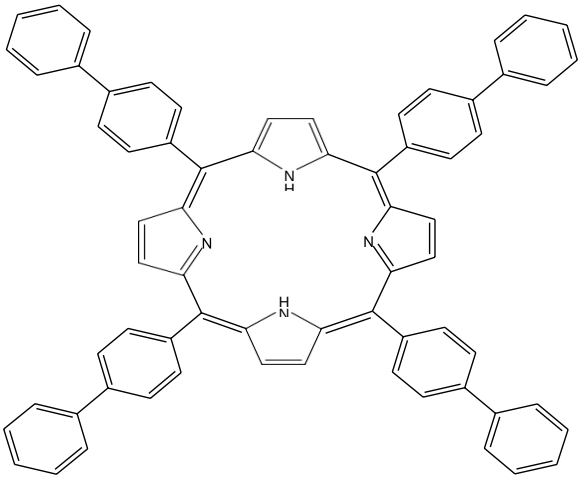

P2 : meso-tetrabiphenyl-porphyrin

$TbiPPH_2$($C_{68}H_{46}N_4$)

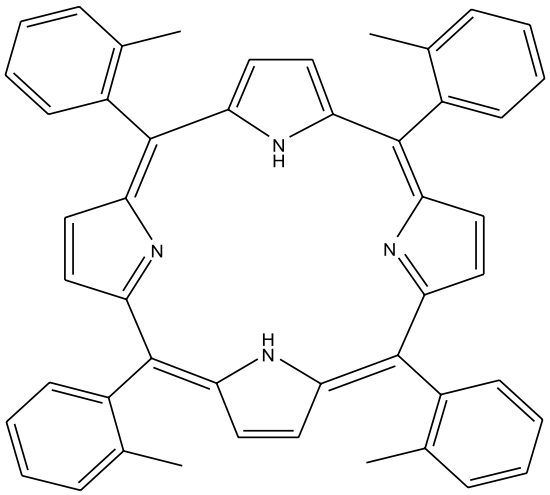

P3: meso-tetramethophenyl-porphyrin

$TPPH_2$ (o-methyl) ($C_{48}H_{38}N_4$)

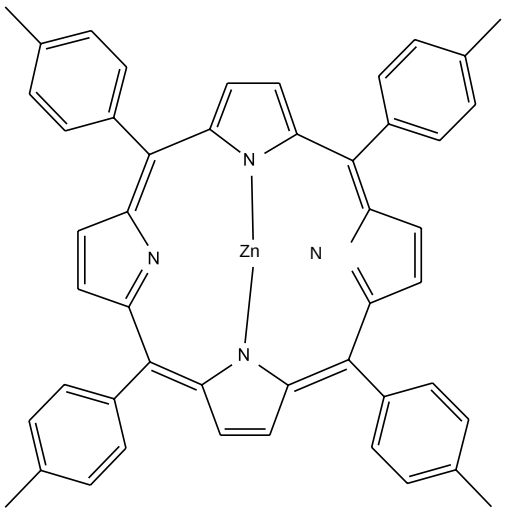

P4: Zinctetra4-methophenyl-porphyrin

$ZnTPPH_2$ (p-methyl) ($C_{48}H_{36}N_4Zn$)

Figure II.1. The chemical formula of the porphyrin derivatives studied.[91]

All porphyrin derivatives were synthesized in accordance with the research conducted by Kadri Mohamed and his scientific team. [92].

3. UV-Vis Spectroscopic Study of HHb Interaction

3.1 Determination of IC_{50} values

In this analysis, the binding interaction between hemoglobin (HHb) and the porphyrin derivatives $NiTPPH_2$, $TbiPPH_2$, $TPPH_2$ (o-methyl), and $ZnTPPH_2$ (p-methyl) was investigated using UV-Vis spectroscopy. The spectroscopic profiles were obtained by measuring absorbance changes upon incremental addition of the porphyrin derivatives to a fixed concentration of HHb.

To assess the binding affinity and determine IC_{50} values, absorbance data were plotted as a function of porphyrin concentration. The interaction was quantified using the following linear equation:

$$\% \text{ inhibition} = \frac{A_0 - A}{A_0} x100 \qquad \text{III. 7}$$

Where A_0 and A represent the absorbance of HHb in the absence and presence of the porphyrin derivative, respectively.

The linear regression equations derived from the absorbance data for each porphyrin compound are summarized in **Table II.1**, alongside their correlation coefficients (R^2) and calculated IC_{50} values:

Table II.1. IC_{50} values (µg/ml) for HHb interaction obtained via UV-Vis spectroscopy.

Compound	Equation	R^2	IC_{50} (µg/ml)
$NiTPPH_2$	y = 1428.172x + 5.631	0.997	31.07
$TbiPPH_2$	y = 1463.746x + 8.222	0.967	28.57
$TPPH_2$ (o-methyl)	y = 1285.518x + 2.067	0.995	37.28
$ZnTPPH_2$ (p-methyl)	y = 1024.681x + 2.914	0.993	45.95

All four compounds demonstrated binding activity with HHb, with distinct variations in their IC_{50} values. The relative binding potency is graphically presented in Figure II.2.

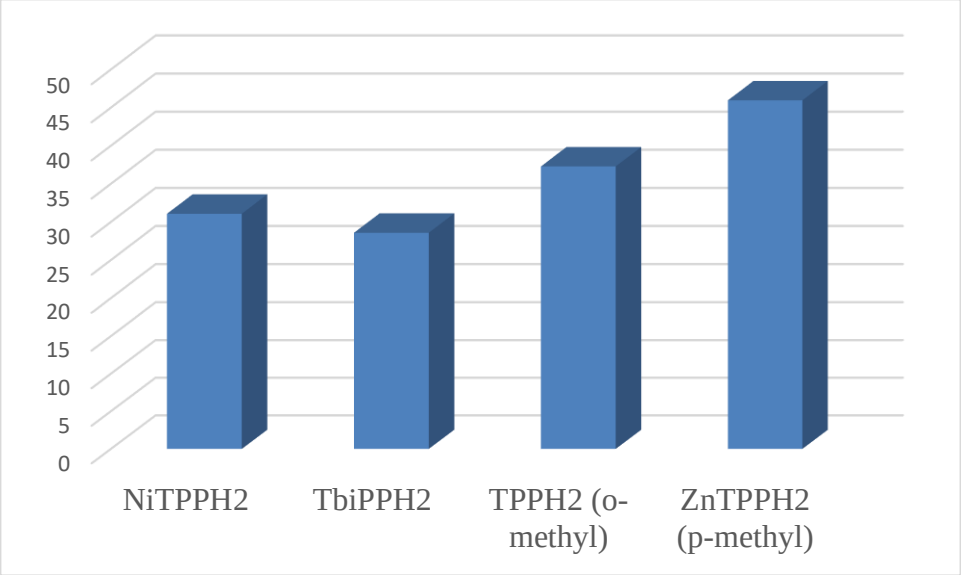

Figure II.2. Classification of HHb inhibition capacity based on IC_{50} values.

From these results, $TbiPPH_2$ exhibited the highest binding affinity (lowest IC_{50} = 28.57 µg/ml), followed by $NiTPPH_2$ (31.07 µg/ml) and $TPPH_2$ (o-methyl) (37.28 µg/ml). $ZnTPPH_2$ (p-methyl) demonstrated the weakest interaction with HHb (IC_{50} = 45.95 µg/ml), indicating that a higher concentration is required to achieve significant inhibition.

These findings suggest that structural differences among the porphyrin derivatives influence their binding efficiency with hemoglobin.

3.2 Binding constants

Figure I.3 illustrates a significant decrease in absorbance with the incremental addition of various concentrations of $NiTPPH_2$, $TbiPPH_2$, $TPPH_2$ (o-methyl), and $ZnTPPH_2$ (p-methyl) into the HHb solution.

This demonstrates a clear correlation between absorbance and the concentration of the porphyrin derivatives, suggesting interaction with hemoglobin.

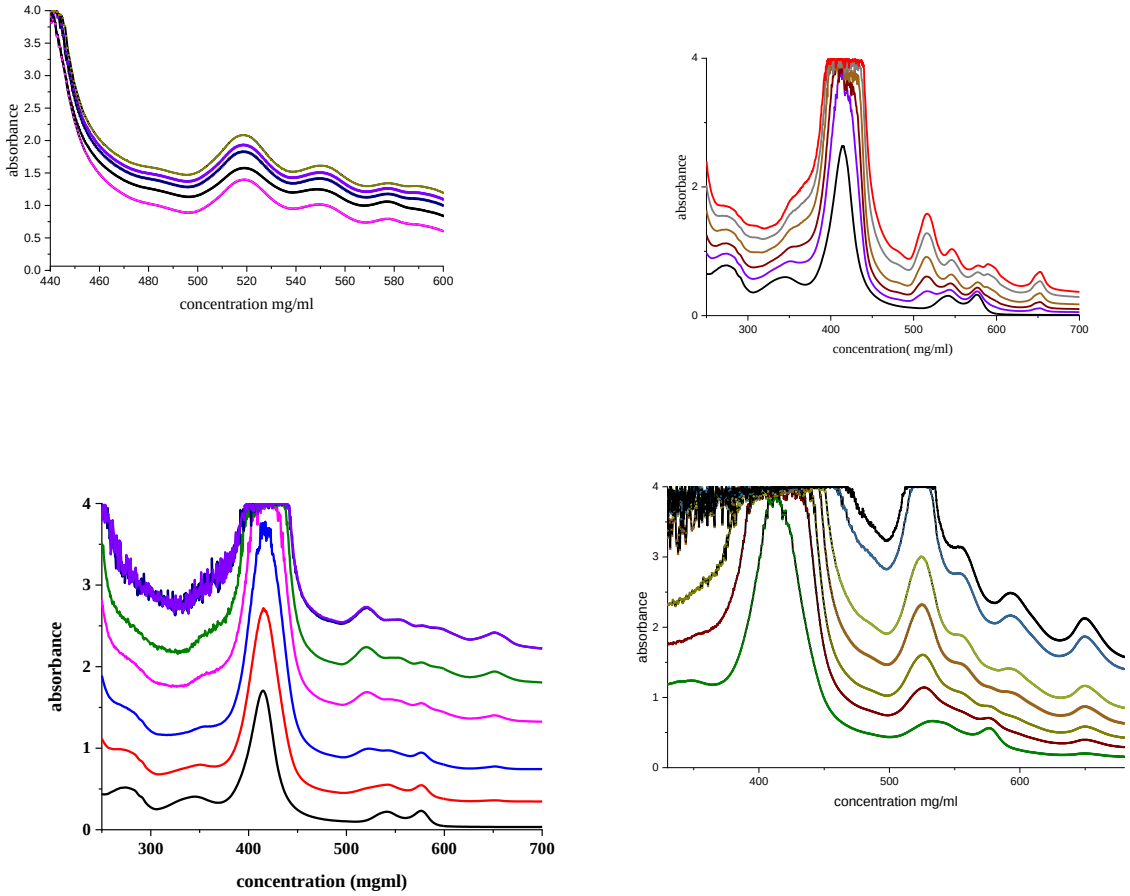

Figure I.3. UV-visible absorption spectra of HHb in the presence of increasing concentrations of NiTPPH2 (A), TbiPPH2 (B), TPPH2 (o-methyl) (C), and ZnTPPH2 (p-methyl) (D) in Acetonitrile at 298 K.

The variation in absorbance values with increasing concentrations of NiTPPH2, TbiPPH2, TPPH2 (o-methyl), and ZnTPPH2 (p-methyl) was used to determine the binding constant (Kb) by applying Equation III.8:

$$\frac{A_0}{A - A_0} = \frac{\varepsilon_G}{\varepsilon_{H-G} - \varepsilon_G} + \frac{\varepsilon_G}{\varepsilon_{H-G} - \varepsilon_G} \frac{1}{K_b [ligand]} \qquad III.8$$

where: [ligand]: is the concentration of the studied compound,

Kb: is the binding constant,

A_0 and A: are respectively the absorbance of HHb in the absence and presence of $NiTPPH_2$, $TbiPPH_2$, $TPPH_2$ (o-methyl), $ZnTPPH_2$ (p-methyl), the studied compounds

ε_G and ε_{G-H}: are their extinction coefficient respectively.

The constant K_b is obtained from the intercept to slope ratio of the plot of $A_0/(A-A_0)$ versus$1/[ligand]$, Figure I.4.

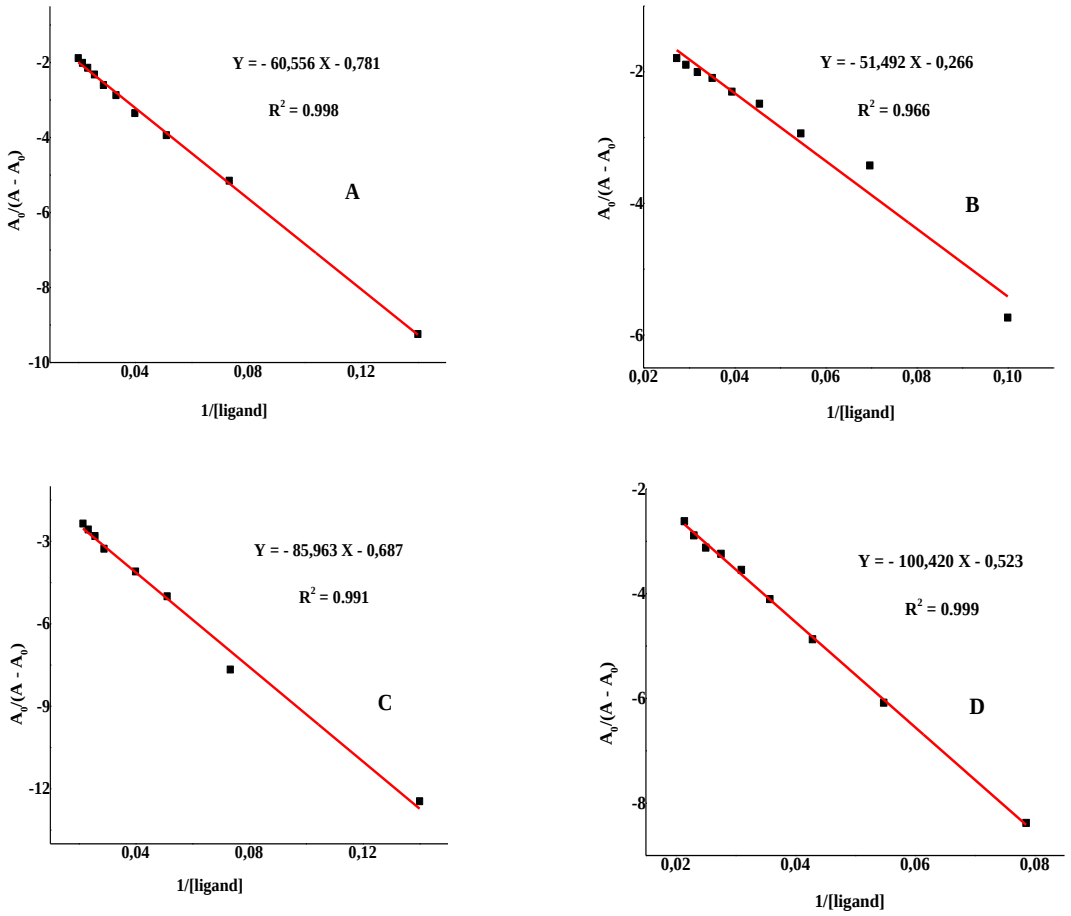

Figure I.4. Plots of $A_0/(A-A_0)$ versus 1/[ligand]1 used to calculate the binding constants of $NiTPPH_2$ (A), $TbiPPH_2$ (B), $TPPH_2$ (o-methyl) (C), and $ZnTPPH_2$ (p-methyl) (D) with HHb.

3.3 Binding Free Energy

The change in free binding energy (ΔG) was calculated using Equation III.3, and the results are presented in Table II.2.

Table II.2 Binding constant and binding free energy values for $NiTPPH_2$, $TbiPPH_2$, $TPPH_2$ (o-methyl), and $ZnTPPH_2$ (p-methyl) ligands with HHb from UV spectroscopy at T = 298 K.

Adduct	Equation	R^2	K (M^{-1})	-ΔG ($kJ \cdot mol^{-1}$)
HHb - NiTPPH2	Y = -60.556X - 0.781	0.998	12.9×10^3	23.47
HHb - TbiPPH2	Y = -51.492X - 0.266	0.966	5.16×10^3	21.19
HHb - TPPH2 (o-Me)	Y = -85.963X - 0.687	0.991	8×10^3	22.28
HHb - ZnTPPH2 (p-Me)	Y = -100.42X - 0.523	0.999	5.21×10^3	21.22

The binding free energy values are relatively similar, suggesting that all four porphyrin derivatives interact with HHb through comparable modes—possibly via nitrogen coordination

to the heme center. $NiTPPH_2$ exhibited the most favorable interaction, indicating its stronger binding affinity to HHb.

Overall, the calculated ΔG values offer meaningful insights into the thermodynamic profiles of the ligand–HHb interactions, with implications for their potential biological relevance.

3.4 Anti-Hemolytic Activity Assessment

In this study, the anti-hemolytic potential of $NiTPPH_2$, $TbiPPH_2$, $TPPH_2$ (o-methyl), and $ZnTPPH_2$ (p-methyl) was evaluated by monitoring hemoglobin release at a single wavelength (540 nm), corresponding to the maximum absorbance of free hemoglobin in hemolyzed erythrocyte suspensions. The percentage of hemolysis inhibition was calculated at different compound concentrations to assess their protective effect against hemolysis.

The inhibition percentage was determined using the following formula:

$$\%\ \text{inhibition} = \frac{A_0 - A}{A_0} x100 \qquad \text{III. 7}$$

Where A_0 and A: are the absorbance of the fully hemolyzed sample in the absence and presence of $NiTPPH_2$, $TbiPPH_2$, $TPPH_2$ (o-methyl), and $ZnTPPH_2$ (p-methyl) respectively.

The data obtained were fitted using a nonlinear exponential regression model to determine the IC_{50} values—the concentrations required to inhibit 50% of hemolysis. Figure I.5 presents the inhibition curves obtained for each compound.

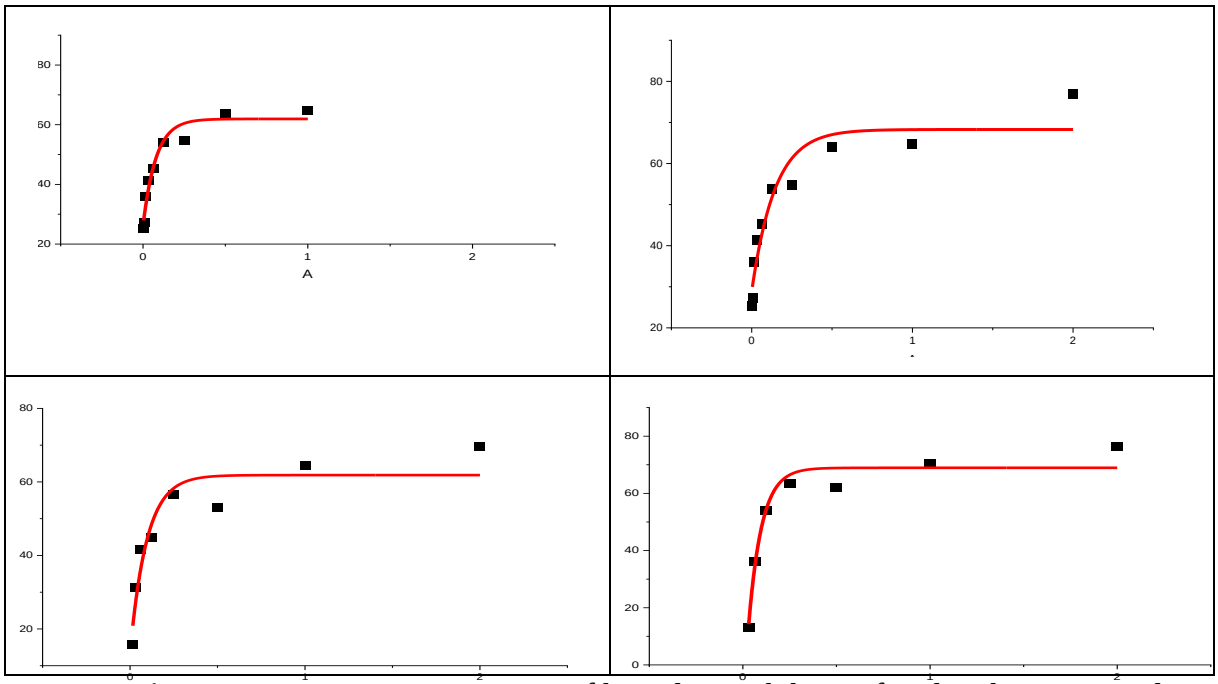

Figure I.5. Dose-response curves of hemolysis inhibition fitted with exponential regression for $NiTPPH_2$ (A), $TbiPPH_2$ (B), $TPPH_2$ (o-methyl) (C), and $ZnTPPH_2$ (p-methyl) (D).

Table II.3 summarizes the IC_{50} values, regression equations, and correlation coefficients (R^2) for each compound.

Table II.3. IC_{50} values, regression equations, and R^2 for the anti-hemolytic activity of porphyrin derivatives.

Compound	R^2	IC_{50} (µM)
$NiTPPH_2$	0.994	14.58
$TbiPPH_2$	0.987	19.23
$TPPH_2$ (o-methyl)	0.991	17.12
$ZnTPPH_2$ (p-methyl)	0.989	20.67

The IC_{50} values obtained for the anti-hemolytic activity of the four porphyrin derivatives, as shown in Table II.3, provide clear insight into their protective efficacy against red blood cell lysis. All compounds demonstrated a dose-dependent inhibitory effect, as reflected by the exponential decay equations with high correlation coefficients ($R^2 > 0.98$), confirming the robustness and reliability of the regression models used.

Among the studied compounds, $NiTPPH_2$ exhibited the lowest IC_{50} value (14.58 µM), indicating the highest anti-hemolytic potency. This suggests a stronger interaction with erythrocyte membranes or enhanced radical-scavenging ability, which could mitigate oxidative damage more effectively than the other derivatives. The corresponding R^2 value of 0.994 supports a strong fit to the model, reinforcing the confidence in this finding.

$TPPH_2$ (o-methyl) followed with an IC_{50} of 17.12 µM, also showing substantial hemolysis inhibition, while $TbiPPH_2$ and $ZnTPPH_2$ (p-methyl) demonstrated moderate activity, with IC_{50} values of 19.23 µM and 20.67 µM, respectively. Despite their similar structural framework, subtle differences in substitution patterns (e.g., presence of methyl or metal centers) appear to influence the compounds' interactions with cellular components, potentially affecting membrane stability or oxidative stress modulation.

Conclusion

Conclusion

This study presents a comprehensive investigation into the potential of nickel (II) and zinc (II) porphyrin complexes as drugs for stabilizing hemoglobin and preventing hemolysis. Our results, obtained through a series of rigorous in vitro experiments and advanced computational simulations, demonstrate the significant potential of these compounds in preventing the degradation of hemoglobin molecules and the lysis of red blood cells under laboratory experimental conditions.

The in vitro experiments revealed that the synthesized porphyrin complexes possess a highly pronounced anti-hemolytic activity, making them suitable therapeutic or prophylactic agents for treating or preventing conditions in which hemolysis plays a significant physiological pathogenic role. Furthermore, the ability of these compounds to stabilize hemoglobin offers promising prospects for their deployment in protecting the integrity of stored blood, which could be applied in medical blood transfusion uses.

Moreover, ADMET predictions provided valuable insights into the presumed pharmacological activity of these compounds, suggesting that they may have a favorable safety and efficacy profile for biological applications. Molecular docking and molecular dynamics analyses supported these findings, showing stable interactions between the porphyrin complexes and the hemoglobin molecule, thus offering a molecular-level explanation for the mechanism through which these compounds stabilize and protect hemoglobin.

The very high efficiency demonstrated by these compounds across various study parameters highlights the importance of designing and synthesizing metalloporphyrin molecules as a potential strategy toward developing new treatments to combat hemolysis and enhance hemoglobin stability. However, it is important to note that these observations are preliminary, and further research—such as bioanalysis and clinical trials—will be necessary to fully assess the efficacy and safety of these compounds before they can be translated into clinical applications.

In conclusion, the study is of great value in clarifying the role of nickel (II) and zinc (II) porphyrin complexes in stabilizing hemoglobin and controlling hemolysis. The promising results achieved open new opportunities for research and development in this field, which could potentially lead to the development of novel therapeutic approaches to improve the health of patients suffering from hemoglobin instability and hemolysis.

References

References

[1] Bruckner, C. (2016). The breaking and mending of meso-tetraarylporphyrins:

Transmuting the pyrrolic building blocks. Accounts of Chemical Research, 49(6), 1080-1092

[2] Li, X. Y., & Zgierski, M. Z. (1991). Porphine force field: in-plane normal modes of free-base porphine; comparison with metalloporphines and structural implications. The Journal of Physical Chemistry, 95(11), 4268-4287

[3] Yin, Q., Alexandrov, E. V., Si, D. H., Huang, Q. Q., Fang, Z. B., Zhang, Y., ... & Proserpio, D. M. (2022). Metallization-Prompted Robust Porphyrin-Based Hydrogen-Bonded Organic Frameworks for Photocatalytic CO2 Reduction. Angewandte Chemie, 134(6), e202115854

[4] Gjuroski, I., Furrer, J., & Vermathen, M. (2021). Probing the interactions of porphyrins with macromolecules using NMR spectroscopy techniques. Molecules, 26(7), 1942

[5] Liu, B., Fu, H., Guan, J., Shao, B., Meng, S., Guo, J., & Wang, W. (2017). An iron-porphyrin complex with large easy-axis magnetic anisotropy on metal substrate. ACS nano, 11(11), 11402-11408

[6] Stępień, M., Sprutta, N., & Latos-Grażyński, L. (2011). Figure eights, Möbius bands, and more: conformation and aromaticity of porphyrinoids. Angewandte Chemie International Edition, 50(19), 4288-4340

[7] Rachlewicz, K., Latos-Grażyński, L., Vogel, E., Ciunik, Z., & Jerzykiewicz, L. B. (2002). Five-coordinate iron (III) porphycenes: 1H NMR, magnetic, and structural studies. Inorganic chemistry, 41(7), 1979-1988

[8] Lammer, A. D. (2018). Novel reactivity of materials from porphyrins, and highly conjugated scaffolds (Doctoral dissertation)

[9] Jasat, A., & Dolphin, D. (1997). Expanded porphyrins and their heterologs. Chemical reviews, 97(6), 2267-2340

[10] Riba López, D. (2023). Synthesis of T-shaped molecules for their deposition over three-terminal device

[11] Hooper, R. W., Zhang, A., Koszelewski, D., Lewtak, J. P., Koszarna, B., Levy, C. J., ... & Stillman, M. J. (2018). Differential quenching of the angular momentum of the B and Q

bands of a porphyrin as a result of extended ring π-conjugation. Journal of Porphyrins and Phthalocyanines, 22(12), 1111-1128 .

[12] Malthus, S. J., Cameron, S. A., & Brooker, S. (2016). First row transition metal complexes of di-o-substituted-diarylamine-based ligands (including carbazoles, acridines and dibenzoazepines). Coordination Chemistry Reviews, 316, 125-161.

[13] Hashimoto, T., Choe, Y. K., Nakano, H., & Hirao, K. (1999). Theoretical study of the Q and B bands of free-base, magnesium, and zinc porphyrins, and their derivatives. The Journal of Physical Chemistry A, 103(12), 1894-1904.

[14-17] Guilard, R., Lecomte, C., & Kadish, K. M. (1987). Synthesis, electrochemistry, and structural properties of porphyrins with metal-carbon single bonds and metal-metal bonds. In Metal Complexes with Tetrapyrrole Ligands I (pp. 205-268). Springer Berlin Heidelberg.

[18] Dolphin, D., & Felton, R. H. (1974). Biochemical significance of porphyrin. pi. cation radicals. Accounts of Chemical Research, 7(1), 26-32.

[19-20] Gu, S., Marianov, A. N., Lu, T., & Zhong, J. (2023). A review of the development of porphyrin-based catalysts for electrochemical CO2 reduction. Chemical Engineering Journal, 470, 144249.

[21] Rachlewicz, K., & Latos-Grażyński, L. (1996). Disproportionation of Iron (III) Porphyrin π-Cation Radicals in the Presence of Sterically Hindered Pyridines. Spectroscopic Detection of Asymmetric Highly Oxidized Intermediates. Inorganic chemistry, 35(5), 1136-1147.

[22]Sun, Z., Jiao, S., Li, F., Wen, J., Yu, Y., Liu, Y., ... & She, Y. (2019). Acid activation and chemical oxidation in the synthesis of meso-tetraphenylporphyrin using a mixed-solvent system. Asian Journal of Organic Chemistry, 8(4), 542-548.

[23] Masa, J., Ozoemena, K. I., Schuhmann, W., & Zagal, J. H. (2013). Fundamental studies on the electrocatalytic properties of metal macrocyclics and other complexes for the electroreduction of O2. In Electrocatalysis in Fuel Cells: A Non-and Low-Platinum Approach (pp. 157-212). London: Springer London.

[24]Fuhrhop, J. H., & Mauzerall, D. (1969). One-electron oxidation of metalloporphyrins. Journal of the American Chemical Society, 91(15), 4174-4181.

[25] Hogan, C. F., Harris, A. R., Bond, A. M., Sly, J., & Crossley, M. J. (2006). Electrochemical studies of porphyrin-appended dendrimers. Physical Chemistry Chemical Physics, 8(17), 2058-2065.

[26] Mu, X. H., Lin, X. Q., & Kadish, K. M. (1989). Microvoltammetric and spectroelectrochemical studies of (TPP) Co oxidation/reduction in toluene and benzene solutions. Electroanalysis, 1(2), 113-116.

[27] Rothemund, P. W. (2000). Using lateral capillary forces to compute by self-assembly. Proceedings of the National Academy of Sciences, 97(3), 984-989.

[28-31] Grzybowski, M., & Gryko, D. T. (2015). Diketopyrrolopyrroles: synthesis, reactivity, and optical properties. Advanced Optical Materials, 3(3), 280-320.

[32] Adler, A. D., Longo, F. R., Finarelli, J. D., Goldmacher, J., Assour, J., & Korsakoff, L. (1967). A simplified synthesis for meso-tetraphenylporphine. The Journal of Organic Chemistry, 32(2), 476-476.

[33-36] Crossley, M. J., Thordarson, P., Bannerman, J. P., & Maynard, P. J. (1998). A convenient procedure for moderate-scale Rothemund synthesis of lipophilic porphyrins: an alternative to the Adler–Longo and Lindsey methodologies. Journal of Porphyrins and Phthalocyanines, 2(6), 511-516.

[37] Lindsey, J. S., & Woodford, J. N. (1995). A simple method for preparing magnesium porphyrins. Inorganic Chemistry, 34(5), 1063-1069.

[38] Cooper, T. W., Campbell, I. B., & Macdonald, S. J. (2010). Factors determining the selection of organic reactions by medicinal chemists and the use of these reactions in arrays (small focused libraries). Angewandte Chemie International Edition, 49(44), 8082-8091.

[39] Pereira, M. M., Pinto, S. M., & Dias, L. D. (2024). Synthesis of Pyrrol-based Bioconjugates: Perspectives and Applications. CRC Press.

[40] Rouvray, D. H. (1974). Isomer enumeration methods. Chemical Society Reviews, 3(3), 355-372.

[41] MacDonald, J. K. L. (1933). Successive approximations by the Rayleigh-Ritz variation method. Physical Review, 43(10), 830.

[42] Balakrishna, A., Aguiar, A., Sobral, P. J., Wani, M. Y., Almeida e Silva, J., & Sobral, A. J. (2019). Paal–Knorr synthesis of pyrroles: from conventional to green synthesis. Catalysis Reviews, 61(1), 84-110.

[43] Schmidt, R. R. (1986). New methods for the synthesis of glycosides and oligosaccharides—are there alternatives to the Koenigs-Knorr method?[New synthetic methods (56)] Angewandte Chemie International Edition in English, 25(3), 212-235.

[44] Bobál, P., & Lightner, D. A. (2001). An improved coupling procedure for the barton-zard pyrrole synthesis. Journal of Heterocyclic Chemistry, 38(2), 527-530.

[45] Bobál, P., & Lightner, D. A. (2001). An improved coupling procedure for the barton-zard pyrrole synthesis. Journal of Heterocyclic Chemistry, 38(2), 527-530.

[46] Singh, A. P., Maurya, N. K., Saxena, R., & Saxena, S. (2024). An overview of red blood cell properties and functions. J Int Res Med Pharm Sci, 19(2), 14-23.

[47] Singh, A. P., Maurya, N. K., Saxena, R., & Saxena, S. (2024). An overview of red blood cell properties and functions. J Int Res Med Pharm Sci, 19(2), 14-23.

[48] Chevrier, B., Weiss, R., Lange, M., Chottard, J. C., & Mansuy, D. (1981). An iron (III)-porphyrin complex with a vinylidene group inserted into an iron-nitrogen bond: Relevance to the structure of the active oxygen complex of catalase. Journal of the American Chemical Society, 103(10), 2899-2901.

[49] Yuan, Y., Tam, M. F., Simplaceanu, V., & Ho, C. (2015). New look at hemoglobin allostery. Chemical reviews, 115(4), 1702-1724.

[50] Gomez-Cambronero, J. (2001). The oxygen dissociation curve of hemoglobin: bridging the gap between biochemistry and physiology. Journal of chemical education, 78(6), 757.

[51] Stark, B. C., Dikshit, K. L., & Pagilla, K. R. (2012). The biochemistry of Vitreoscilla hemoglobin. Computational and structural biotechnology journal, 3(4), e201210002.

[52] Stark, B. C., Dikshit, K. L., & Pagilla, K. R. (2012). The biochemistry of Vitreoscilla hemoglobin. Computational and structural biotechnology journal, 3(4), e201210002.

[53] Stark, B. C., Dikshit, K. L., & Pagilla, K. R. (2012). The biochemistry of Vitreoscilla hemoglobin. Computational and structural biotechnology journal, 3(4), e201210002.

[54] Carlsen, C. U., Møller, J. K., & Skibsted, L. H. (2005). Heme-iron in lipid oxidation. Coordination Chemistry Reviews, 249(3-4), 485-498.

[55] Gupta, A. S. (2019). Hemoglobin-based oxygen carriers: current state-of-the-art and novel molecules. Shock, 52(1S), 70-83.

[56] Cantu-Medellin, N., Vitturi, D. A., Rodriguez, C., Murphy, S., Dorman, S., Shiva, S., ... & Patel, R. P. (2011). Effects of T-and R-state stabilization on deoxyhemoglobin-nitrite reactions and stimulation of nitric oxide signaling. Nitric Oxide, 25(2), 59-69.

[57] Bozza, M. T., & Jeney, V. (2020). Pro-inflammatory actions of heme and other hemoglobin-derived DAMPs. Frontiers in immunology, 11, 1323.

[58] Vaupel, P., Mayer, A., & Höckel, M. (2006). Impact of hemoglobin levels on tumor oxygenation: the higher, the better?. Strahlentherapie und Onkologie, 182(2), 63-71.

[59] Rifkind, J. M., Nagababu, E., Ramasamy, S., & Ravi, L. B. (2003). Hemoglobin redox reactions and oxidative stress. Redox report, 8(5), 234-237.

[60] Uríčková, V., & Sádecká, J. (2015). Determination of geographical origin of alcoholic beverages using ultraviolet, visible and infrared spectroscopy: A review. Spectrochimica Acta Part A: Molecular and Biomolecular Spectroscopy, 148, 131-137.

[61] Zhou, H., Peng, J., Duan, X., Yin, H., Huang, B., Zhou, C., ... & Lai, B. (2023). Redox-active polymers as robust electron-shuttle co-catalysts for fast Fe3+/Fe2+ circulation and green fenton oxidation. Environmental Science & Technology, 57(8), 3334-3344.

[62] Knirsch, M. C., Dell'Anno, F., Salerno, M., Larosa, C., Polakiewicz, B., Eggenhöffner, R., & Converti, A. (2017). Combined characterization of bovine polyhemoglobin microcapsules by UV–Vis absorption spectroscopy and cyclic voltammetry. Bioprocess and biosystems engineering, 40, 431-438.

[63] Fattizzo, B., & Barcellini, W. (2022). Autoimmune hemolytic anemia: causes and consequences. Expert review of clinical immunology, 18(7), 731-745.

[64] Gladwin, M. T., Kanias, T., & Kim-Shapiro, D. B. (2012). Hemolysis and cell-free hemoglobin drive an intrinsic mechanism for human disease. The Journal of clinical investigation, 122(4), 1205-1208.

[65] Fibach, E., & Rachmilewitz, E. (2008). The role of oxidative stress in hemolytic anemia. Current molecular medicine, 8(7), 609-619.

[66] Naeem, N., Drese, K. S., Paterson, L., & Kersaudy-Kerhoas, M. (2021). Current and emerging microfluidic-based integrated solutions for free hemoglobin and hemolysis detection and measurement. Analytical Chemistry, 94(1), 75-85.

[67] Ascenzi, P., Bocedi, A., Visca, P., Altruda, F., Tolosano, E., Beringhelli, T., & Fasano, M. (2005). Hemoglobin and heme scavenging. IUBMB life, 57(11), 749-759.

[68] Safo, M. K., Ahmed, M. H., Ghatge, M. S., & Boyiri, T. (2011). Hemoglobin–ligand binding: Understanding Hb function and allostery on atomic level. Biochimica et Biophysica Acta (BBA)-Proteins and Proteomics, 1814(6), 797-809.

[69] Joshi, T., Graham, B., & Spiccia, L. (2015). Macrocyclic metal complexes for metalloenzyme mimicry and sensor development. Accounts of chemical research, 48(8), 2366-2379.

[70] Scheidt, W. R., & Ellison, M. K. (1999). The synthetic and structural chemistry of heme derivatives with nitric oxide ligands. Accounts of chemical research, 32(4), 350-359.

[71] Mao, L., Song, Q., Li, M., Liu, X., Shi, Z., Chen, F., ... & Zhu, X. G. (2023). Decreasing photosystem antenna size by inhibiting chlorophyll synthesis: A double-edged sword for photosynthetic efficiency. Crop and Environment, 2(1), 46-58.

[72] Kato, H., Komagoe, K., Inoue, T., Masuda, K., & Katsu, T. (2018). Structure—Activity relationship of porphyrin-induced photoinactivation with membrane function in bacteria and erythrocytes. Photochemical & Photobiological Sciences, 17, 954-963.

[73] Tsoupras, A., Pafli, S., Stylianoudakis, C., Ladomenou, K., Demopoulos, C. A., & Philippopoulos, A. (2024). Anti-inflammatory and antithrombotic potential of metal-based complexes and porphyrins. Compounds, 4(2), 376-400.

[74] Alomari, E. A. A. M. (2020). Protein therapeutics for clinical applications: Hemoglobin-based oxygen carriers and modulation of their oxygen-binding properties.

[75] Zhao, Y., Wang, Y., Ran, F., Cui, Y., Liu, C., & Gao, Y. (2018). Hemolysis and cytotoxicity assays for biomaterials. International Journal of Nanomedicine, 13, 8445–8455

[76] Hu, C.-M. J., Zhang, L., Aryal, S., Cheung, C., Fang, R. H., & Zhang, L. (2011). Erythrocyte membrane-camouflaged polymeric nanoparticles as a biomimetic delivery platform. Proceedings of the National Academy of Sciences, 108(27), 10980.10985.

[77] Kaabi, I., Amamra, S., Douadi, T., Al-Noaimi, M., Chafai, N., Boublia, A., ... & Benguerba, Y. (2024). Unveiling the dual role of a novel azomethine: Corrosion inhibition and antioxidant potency–a multifaceted study integrating experimental and theoretical approaches. Journal of the Taiwan Institute of Chemical Engineers, 161, 105535.

[78] Benesi, H. A., & Hildebrand, J. H. (1949). A spectrophotometric investigation of the interaction of iodine with aromatic hydrocarbons. Journal of the American Chemical Society, 71(8), 2703–2707.

[79] Rashid, M. A. M., Rahman, M., Mahmud, A. O., Morshed, A. S. M., Haque, M. M., & Hossain, M. M. (2022). UV-vis spectrophotometer as an alternative technique for the determination of hydroquinone in vinyl acetate monomer. Photochem, 2(2), 435-447.

[80] Liu, Y., Lin, J., Chen, M., & Song, L. (2013). Investigation on the interaction of the toxicant, gentian violet, with bovine hemoglobin. Food and chemical toxicology, 58, 264-272.

[81] Liu, Y., Wen, N., Li, K., Li, M., Qian, S., Li, S., ... & Liu, Z. (2022). Photolytic removal of red blood cell membranes camouflaged on nanoparticles for enhanced cellular uptake and combined chemo-photodynamic inhibition of cancer cells. Molecular Pharmaceutics, 19(3), 805-818.

[82] Benesi, H. A., & Hildebrand, J. H. (1949). A spectrophotometric investigation of the interaction of iodine with aromatic hydrocarbons. Journal of the American Chemical Society, 71(8), 2703–2707.

[83] Krzywanski, J., Sosnowski, M., Grabowska, K., Zylka, A., Lasek, L., & Kijo-Kleczkowska, A. (2024). Advanced computational methods for modeling, prediction and optimization—a review. Materials, 17(14), 3521.

[84] Filosa, R., Peduto, A., Di Micco, S., de Caprariis, P., Festa, M., Petrella, A., ... & Bifulco, G. (2009). Molecular modelling studies, synthesis and biological activity of a series of novel bisnaphthalimides and their development as new DNA topoisomerase II inhibitors. Bioorganic & Medicinal Chemistry, 17(1), 13-24.

[85] Ahmad, S., Singh, S., Srivastava, M. R., Shukla, S., Rai, S., & Shamsi, A. S. (2021). Molecular docking simplified: literature review. Adv. Med. Dent. Health Sci, 4, 37-44.

[86] Paquet, E., & Viktor, H. L. (2015). Molecular dynamics, monte carlo simulations, and langevin dynamics: a computational review. BioMed research international, 2015(1), 183918.

[87] Fermeglia, M., & Pricl, S. (2009). Multiscale molecular modeling in nanostructured material design and process system engineering. Computers & Chemical Engineering, 33(10), 1701-1710.

[88] Dykstra, C. E. (1993). Electrostatic interaction potentials in molecular force fields. Chemical Reviews, 93(7), 2339-2353.

[89] Adelusi, T. I., Oyedele, A. Q. K., Boyenle, I. D., Ogunlana, A. T., Adeyemi, R. O., Ukachi, C. D., ... & Abdul-Hammed, M. (2022). Molecular modeling in drug discovery. Informatics in Medicine Unlocked, 29, 100880.

[90] Apra, E., Bylaska, E. J., De Jong, W. A., Govind, N., Kowalski, K., Straatsma, T. P., ... & Harrison, R. J. (2020). NWChem: Past, present, and future. The Journal of chemical physics, 152(18).

[91] Hobbs, C. J. (2017). Development and Application of Porphyrin-Maquette Complexes: Towards Artificial Photosynthesis (Doctoral dissertation, University of Wollongong).

[92] R Soury, A Elamri, M El Oudi, KM Alenezi, M Jabli… - Molecules, 2024 - mdpi.com

[93] Ahmed, A., Omar, W. A., El-Asmy, H. A., Abou-Zeid, L., & Fadda, A. A. (2020). Docking studies, antitumor and antioxidant evaluation of newly synthesized porphyrin and metalloporphyrin derivatives. Dyes and Pigments, 183, 108728.

[94] Yang, Y., Weaver, M. N., & Merz Jr, K. M. (2009). Assessment of the "6-31+ G**+ LANL2DZ" mixed basis set coupled with density functional theory methods and the effective core potential: prediction of heats of formation and ionization potentials for first-row-transition-metal complexes. The Journal of Physical Chemistry A, 113(36), 9843-9851.

[95] DS Metibemu, OA Akinloye, AJ Akamo, JO Okoye, DA Ojo, E Morifi, Journal of Food Biochemistry 44 (12), e13523, 2020.

Annexe

Annexe

UV -1800 UV-Visible Spectrophotometer

sp-v1100 Spectrophotometer

Centrifugation

KERN Precision Balance

Pipette, insulin syringe and tube